Table 3. Alignment of the 16S rRNA, ITS, *hsp65* and *rpoB* gene sequences from 24 piscine isolates and 6 reference strains[a)]

Strain	Prefecture/ Country	Nucleotide sequence positions																			
		16S rRNA[b)]								ITS region				*hsp65*[c)]						*rpoB*[d)]	
		95	487–8	492	969	1007	1215	1247	1288	30	57	62	83	455	571	637	639	647	797	92	143
M. shinshuense ATCC 33728	Nagano/Japan	T	GG	G	A	G	T	G	G	G	G	T	A	C	T	C	C	A	T	C	C
M. ulcerans ATCC 19423^T	NC[e)]/ Australia	T	GG	A	A	G	T	G	C	G	G	T	A	T	C	C	C	A	C	T	C
M. ulcerans Agy99	NC / Ghana	T	GG	A	A	G	T	G	C	G	G	T	A	T	C	C	C	A	C	T	C
M. marinum ATCC 927^T	NC / USA	T	GG	A	A	G	T	A	A	G	G	T	A	C	C	C	T	G	C	C	G
M. marinum 112509	Tokyo/Japan	T	GG	A	A	G	T	A	A	G	G	T	G	C	C	C	T	G	C	C	G
M. pseudoshottsii JCM 15466^T	NC / USA	C	GA	A	G	T	C	A	A	A	G	C	A	C	C	T	C	G	C	C	C
MF01 (yellow tail)	Kagoshima/Japan	C	GA	A	G	T	C	A	A	A	G	C	A	C	C	T	C	G	C	C	C
MF06 (yellow tail)	Kagoshima/Japan	C	GG	A	G	T	C	A	A	A	G	C	A	C	C	T	C	G	C	C	C
MF09 (yellow tail)	Oita/Japan	C	GG	A	G	T	C	A	A	A	T	C	A	C	C	T	C	G	C	C	C
MF10 (yellow tail)	Oita/Japan	C	GA	A	G	T	C	A	A	A	G	C	A	C	C	T	C	G	C	C	C
MF12 (yellow tail)	Ehime/Japan	C	GA	A	G	T	C	A	A	A	G	C	A	C	C	T	C	G	C	C	C
MF14 (yellow tail)	Ehime/Japan	C	AA	A	G	T	C	A	A	A	G	C	A	C	C	T	C	G	C	C	C
MF31 (yellow tail)	Kagoshima/Japan	C	GA	A	G	T	C	A	A	A	G	C	A	C	C	T	C	G	C	C	C
MF32 (yellow tail)	Kagoshima/Japan	C	GA	A	G	T	C	A	A	A	G	C	A	C	C	T	C	G	C	C	C
MF33 (yellow tail)	Kagoshima/Japan	C	GA	A	G	T	C	A	A	A	G	C	A	C	C	T	C	G	C	C	C
MF34 (yellow tail)	Kagoshima/Japan	C	AA	A	G	T	C	A	A	A	T	C	A	C	C	T	C	G	C	C	C
MF35 (yellow tail)	Kagoshima/Japan	C	GA	A	G	T	C	A	A	A	G	C	A	C	C	T	C	G	C	C	C
MF36 (yellow tail)	Kagoshima/Japan	C	GA	A	G	T	C	A	A	A	G	C	A	C	C	T	C	G	C	C	C
MF44 (yellow tail)	Oita/Japan	C	AA	A	G	T	C	A	A	A	T	C	A	C	C	T	C	G	C	C	C
MF45 (yellow tail)	Oita/Japan	C	GA	A	G	T	C	A	A	A	G	C	A	C	C	T	C	G	C	C	C
MF46 (yellow tail)	Ehime/Japan	C	GA	A	G	T	C	A	A	A	G	C	A	C	C	T	C	G	C	C	C
MF02 (greater amberjack)	Kagoshima/Japan	C	GA	A	G	T	C	A	A	A	G	C	A	C	C	T	C	G	C	C	C
MF05 (greater amberjack)	Kagoshima/Japan	C	GG	A	G	T	C	A	A	A	T	C	A	C	C	T	C	G	C	C	C
MF07 (greater amberjack)	Miyazaki /Japan	C	GG	A	G	T	C	A	A	A	G	C	A	C	C	T	C	G	C	C	C
MF40 (greater amberjack)	Kagoshima/Japan	C	GA	A	G	T	C	A	A	A	G	C	A	C	C	T	C	G	C	C	C
MF13 (sevenband grouper)	Ehime/Japan	C	GA	A	G	T	C	A	A	A	G	C	A	C	C	T	C	G	C	C	C
MF15 (sevenband grouper)	Ehime/Japan	C	GA	A	G	T	C	A	A	A	G	C	A	C	C	T	C	G	C	C	C
MF04 (striped jack)	Kagoshima/Japan	C	AA	A	G	T	C	A	A	A	T	C	A	C	C	T	C	G	C	C	C
MF08 (striped jack)	Oita/Japan	C	GG	A	G	T	C	A	A	A	G	C	A	C	C	T	C	G	C	C	C
MF11 (yellowtail amberjack)	Oita/Japan	C	GA	A	G	T	C	A	A	A	G	C	A	C	C	T	C	G	C	C	C

a) Only nucleotide differences are noted. Nucleotide positions were based on the b) *E. coli* 16S rRNA gene (accession No. J01859). c) *M. tuberculosis hsp65* gene. (accession No. M15467) and d) *rpoB* gene (accession No. AF057454). e) Not clear.

lates showed complete identity with those of the *M. pseudoshottsii* sequences (Table 3). A conserved mismatch between piscine and human isolates in *hsp65* gene fragments was only found at nucleotide position 637. The results showed that the 24 piscine isolates were all identified as *M. pseudoshottsii* rather than *M. marinum*.

A lethal case of *M. marinum* in cultured yellowtails, which was identified using biological, biochemical and 16S rRNA sequence analyses, has been reported in Japan [17]. In our study, *M. pseudoshottsii* was identified as an additional source of atypical piscine mycobacteriosis and (the bacteria) had been distributed in farmed fisheries in the west part of Japan since 1999. Further studies are needed to develop an easier method to distinguish *M. pseudoshottsii* from *M. marinum* because both strains might have not been differentiated before in Japan. Their differences in susceptibility to antimicrobial agents and in capacity for human pathogenesis should be elucidated. In addition, *M. pseudoshottsii* produces a unique plasmid-encoded toxic macrolide, mycolactone F [7], suggesting that *M. pseudoshottsii* provides a reservoir in aquatic environments for the horizontal transfer of the plasmid-borne genes that encode mycolactone F. Interestingly the potency of mycolactone F with regard to apoptosis in a mammalian cell line was significantly less than that of mycolactone A/B, which is produced by *M. ulcerans*, a causative agent of Buruli ulcer [17]. Further molecular, biochemical and drug susceptibility studies are needed to understand the possible role of mycolactone F in mycobacteriosis and to fully characterize piscine mycobacterial infections in Japan.

ACKNOWLEDGMENTS. We thank Prof. Yoshida (University of Miyazaki, Japan), Dr. Fukuda (Oita Prefectural Agriculture, Forestry and Fisheries Research Center) and Dr. Yamashita (Ehime Prefectural Agriculture, Forestry and Fisheries Research Center) for providing mycobacterial isolates obtained from affected fishes. This work was supported in part by a Grant-in-Aid for Research on Emerging and Re-emerging Infectious Diseases from the Ministry of Health, Labour, and Welfare of Japan to Y. H., M. M. and N. I., by a Grant-in-Aid for Scientific Research (C) from the Ministry of Education, Culture, Sports, Science and Tech-

nology of Japan to Y. H. and by a Grant-in-Aid for Scientific Research (C) from the Japan Society for the Promotion of Science to K. N.

REFERENCES

1. Chemlal, K. and Portaels, F. 2003. Molecular diagnosis of non-tuberculous mycobacteria. *Curr. Opin. Infect. Dis.* **16**: 77–83.
2. Decostere, A., Hermans, K. and Haesebrouck, F. 2004. Piscine mycobacteriosis: a literature review covering the agent and the disease it causes in fish and humans. *Vet. Microbiol.* **99**: 159–166.
3. Devulder, G., Pérouse de Montclos, M. and Flandrois, J. P. 2005. A multigene approach to phylogenetic analysis using the genus Mycobacterium as a model. *Int. J. Syst. Evol. Microbiol.* **55**: 293–302.
4. Frerichs, G. N. 1993. Mycobacteriosis: nocardiosis. pp. 219–234. *In*: Bacterial Diseases of Fish (Inglis, V., Roberts , R. J. and Bromage, N. R. eds.), Halsted Press, New York.
5. Kim, B. J., Lee, S. H., Lyu, M. A., Kim, S. J., Bai, G. H., Kim, S. J., Chae, G. T., Kim, E. C., Cha, C. Y. and Kook, Y. H. 1999. Identification of mycobacterial species by comparative sequence analysis of the RNA polymerase gene (*rpoB*). *J. Clin. Microbiol.* **37**: 1714–1720.
6. Nakanaga, K., Ishii, N., Suzuki, K., Tanigawa, K., Goto, M., Okabe, T., Imada, H., Kodama, A., Iwamoto, T., Takahashi, H. and Saito, H. 2007. "*Mycobacterium ulcerans* subsp. *shinshuense*" isolated from a skin ulcer lesion: identification based on 16S rRNA gene sequencing. *J. Clin. Microbiol.* **45**: 3840–3843.
7. Pidot, S. J., Hong, H., Seemann, T., Porter, J. L., Yip, M. J., Men, A., Johnson, M., Wilson, P., Davies, J. K., Leadlay, P. F. and Stinear, T. P. 2008. Deciphering the genetic basis for polyketide variation among mycobacteria producing mycolactones. *BMC Genomics* **9**: 462.
8. Ranger, B. S., Mahrous, E. A., Mosi, L., Adusumilli, S., Lee, R. E., Colorni, A., Rhodes, M. and Small, P. L. C. 2006. Globally distributed Mycobacterial fish pathogens produce a novel plasmid-encoded toxic macrolide, mycolactone F. *Infect. Immun.* **74**: 6037–6045.
9. Rhodes, M. W., Kator, H., Kotob, S., van Berkum, P., Kaattari, I., Vogelbein, W., Floyd, M. M., Butler, W. R., Quinn, F. D., Ottinger, C. and Shotts, E. 2001. A unique Mycobacterium species isolated from an epizootic of striped bass (Morone saxatilis). *Emerg. Infect. Dis.* **7**: 896–899.
10. Rhodes, M. W., Kator, H., McNabb, A., Deshayes, C., Reyrat, J., Brown-Elliott, B. A., Wallace, R., Trott, K., Parker, J. M., Lifland, B., Osterhout, G., Kaattari, I., Reece, K., Vogelbein, W. and Ottinger, C. A. 2005. *Mycobacterium pseudoshottsii* sp. nov., a slowly growing chromogenic species isolated from Chesapeake Bay striped bass (Morone saxatilis). *Int. J. Syst. Evol. Microbiol.* **55**: 1139–1147.
11. Roth, A., Fischer, M., Hamid, M. E., Michalke, S., Ludwig, W. and Mauch, H. 1998. Differentiation of phylogenetically related slowly growing mycobacteria based on 16S-23S rRNA gene internal transcribed spacer sequences. *J. Clin. Microbiol.* **36**: 139–147.
12. Springer, B., Wu, W. K., Bodmer, T., Haase, G., Pfyffer, G. E., Kroppenstedt, R. M., Schroder, K. H., Emler, S., Kilburn, J. O., Kirschner, P., Telenti, A., Coyle, M. B. and Böttger, E. C. 1996. Isolation and characterization of a unique group of slowly growing mycobacteria: description of *Mycobacterium lentiflavum* sp. nov. *J. Clin. Microbiol.* **34**: 1100–1107.
13. Stine, C. B., Jakobs, J. M., Rhodes, M. R., Overton, A., Fast, M. and Baya, A. M. 2009. Expanded range and new host species of *Mycobacterium shottsii* and *M. pseudoshottsii*. *J. Aquat. Anim. Health* **21**: 179–183.
14. Stinear, T. P., Mve-Obiang, A., Small, P. L., Frigui, W., Pryor, M. J., Brosch, R., Jenkin, G. A. Johnson, P. D., Davies, J. K., Lee, R. E., Adusumilli, S., Garnier, T., Haydock, S. F., Leadlay, P. F. and Cole, S. T. 2004. Giant plasmid-encoded polyketide synthases produce the macrolide toxin of *Mycobacterium ulcerans*. *Proc. Natl. Acad. Sci. U.S.A.* **101**: 1345–1349.
15. Stragier, P., Hermans, K., Stinear, T. and Portaels, F. 2008. First report of a mycolactone-producing Mycobacterium infection in agriculture in Belgium. *FEMS Microbiol. Lett.* **286**: 93–95.
16. Telenti, A., Marchesi, F., Balz, M., Bally, F., Böttger, E. C. and Bodmer, T. 1993. Rapid identification of mycobacteria to the species level by polymerase chain reaction and restriction enzyme analysis. *J. Clin. Microbiol.* **31**: 175–178.
17. Weerakhun, S., Aoki, N., Kurata, O., Hatai, K., Nibe, H. and Hirae, T. 2007. *Mycobacterium marinum* infection in cultured yellowtail Seriiola quinqueradiata in Japan. *Fish Pathol.* **42**: 79–84.

AAC
Journals.ASM.org

Mutation Analysis of Mycobacterial *rpoB* Genes and Rifampin Resistance Using Recombinant *Mycobacterium smegmatis*

Noboru Nakata, Masanori Kai, and Masahiko Makino

Department of Mycobacteriology, Leprosy Research Center, National Institute of Infectious Diseases, Tokyo, Japan

Rifampin is a major drug used to treat leprosy and tuberculosis. The rifampin resistance of *Mycobacterium leprae* and *Mycobacterium tuberculosis* results from a mutation in the *rpoB* gene, encoding the β subunit of RNA polymerase. A method for the molecular determination of rifampin resistance in these two mycobacteria would be clinically valuable, but the relationship between the mutations and susceptibility to rifampin must be clarified before its use. Analyses of mutations responsible for rifampin resistance using clinical isolates present some limitations. Each clinical isolate has its own genetic variations in some loci other than *rpoB*, which might affect rifampin susceptibility. For this study, we constructed recombinant strains of *Mycobacterium smegmatis* carrying the *M. leprae* or *M. tuberculosis rpoB* gene with or without mutation and disrupted their own *rpoB* genes on the chromosome. The rifampin and rifabutin susceptibilities of the recombinant bacteria were measured to examine the influence of the mutations. The results confirmed that several mutations detected in clinical isolates of these two pathogenic mycobacteria can confer rifampin resistance, but they also suggested that some mutations detected in *M. leprae* isolates or rifampin-resistant *M. tuberculosis* isolates are not involved in rifampin resistance.

Downloaded from http://aac.asm.org/ on March 19, 2012 by NATL INST OF INFECTIOUS DISEAS

Leprosy and tuberculosis persist as important global public health concerns. Rifampin, a major drug used to treat these two infectious diseases, has a molecular mechanism of activity involving the inhibition of DNA-dependent RNA polymerase (15). In *Escherichia coli*, this enzyme is a complex oligomer comprised of four subunits, α, β, β′, and σ, encoded by *rpoA*, *rpoB*, *rpoC*, and *rpoD*, respectively. Rifampin binds to the β subunit of RNA polymerase and results in transcription inhibition (15). Mutations in the *rpoB* gene, encoding the β subunit of RNA polymerase, reportedly result in resistance to rifampin in several mycobacterial species, including *Mycobacterium leprae* and *Mycobacterium tuberculosis* (9, 21). The former has not yet been cultured on artificial media; it requires 11 to 14 days to double in experimentally infected mice. Therefore, it is difficult to determine the rifampin susceptibilities of *M. leprae* isolates. The standardized method using a mouse footpad takes more than half a year to determine the rifampin susceptibility of *M. leprae* isolates and requires 5×10^3 *M. leprae* bacilli (3), which require almost a year to prepare. *In vitro* drug susceptibility testing for *M. leprae* using a radioactive reagent requires more (10^7) *M. leprae* cells (7). In contrast, mutations in the *rpoB* gene of *M. leprae* can be detected in a few days or less. It would be very helpful if mutations responsible for rifampin resistance could be determined without performing mouse footpad testing. The main mutations that confer rifampin resistance to *M. tuberculosis* are located in the 81-bp core region of the *rpoB* gene, encompassing codons 507 to 533, known as the rifampin resistance-determining region (RRDR) (17, 18). About 95% of rifampin-resistant *M. tuberculosis* strains have a mutation in this region (18, 20). Four mutations, D516V, H526Y, H526D, and S531L, are most commonly associated with the high-level rifampin resistance of *M. tuberculosis* strains (4, 10, 19), but some other mutations in the 81-bp region have not yet been confirmed completely as being responsible for rifampin resistance.

We have established a method to determine the mutations responsible for the dapsone resistance of *M. leprae* using recombinant *Mycobacterium smegmatis* strains (16). In the present study, we assessed the applicability of the determination of rifampin resistance for analysis. We then analyzed *rpoB* mutations conferring rifampin resistance to *M. leprae* and *M. tuberculosis*.

MATERIALS AND METHODS

Bacterial strains and plasmids. *E. coli* DH5α was used for DNA cloning. *M. smegmatis* mc^{2}155 was used as a mycobacterial host to produce strains for drug susceptibility testing. Plasmids pYUB854 and phAE87 were kindly provided by W. R. Jacobs, Jr. (Department of Microbiology and Immunology, Albert Einstein College of Medicine, New York, NY). *M. smegmatis* mc^{2}155 and its transformants were grown in Middlebrook 7H9 medium (Difco Laboratories, Detroit, MI) supplemented with 0.5% bovine serum albumin (fraction V), 0.2% glucose, 0.085% NaCl, 0.2% glycerol, and 0.1% Tween 80.

Site-directed mutagenesis. The wild-type *rpoB* genes of *M. leprae* and *M. tuberculosis* were amplified from *M. leprae* Thai-53 and *M. tuberculosis* H37Rv by PCR and cloned into pMV261. Site-directed mutagenesis was performed by using PCR with DNA polymerase (Takara PrimeStar HS; Takara Bio Inc., Kyoto, Japan) and the primers presented in Table 1. PCR products were purified and phosphorylated with T4 kinase and ATP and were then ligated to make them circular. The ligation mixture was used to transform *E. coli* DH5α cells, and kanamycin-resistant colonies were isolated. Plasmids were extracted from the transformants. The mutated sequences were then confirmed by sequencing. The inserts of the plasmids were also cloned into pNN301 (16). Mutations introduced into the *M. leprae rpoB* or *M. tuberculosis rpoB* gene are listed in Table 2.

Disruption of the *rpoB* gene on the *M. smegmatis* chromosome. *M. smegmatis* mc^{2}155 cells were transformed with plasmids carrying the *M. leprae* or *M. tuberculosis rpoB* gene with or without a point mutation. Recombinants were selected on LB medium containing kanamycin. Allel-

Received 30 September 2011 Returned for modification 31 October 2011
Accepted 4 January 2012
Published ahead of print 17 January 2012
Address correspondence to Noboru Nakata, n-nakata@nih.go.jp.
Supplemental material for this article may be found at http://aac.asm.org/.
Copyright © 2012, American Society for Microbiology. All Rights Reserved.
doi:10.1128/AAC.05831-11

TABLE 1 Primers used for this study

Primer	Sequence[a]	Application
M. smegmatis		
MSRBUF	GCCTTAAGGAGGAGAAGGACGAGGCCAC	*rpoB* disruption, upstream forward
MSRBUR	GCTCTAGACAAGATGCATCCTTCCAGCA	*rpoB* disruption, upstream reverse
MSRBDF	GCAAGCTTTCGCGCAACGAATCCGCGTC	*rpoB* disruption, downstream forward
MSRBDR	GCACTAGTAGCGCACGCAGCTTCTTCTG	*rpoB* disruption, downstream reverse
MSRBF	TGGTCAAGCAGTTCCTCAAC	Detection of *rpoB* disruption, forward
MSRBR	CGTTGTTGACGATGATCTCG	Detection of *rpoB* disruption, reverse
M. leprae		
MLRBWTF	GCGGATCCGTGCTGGAAGGATGCATCTT	Cloning of *M. leprae rpoB*, forward
MLRBWTR	GCGTTAACCTAAGCCAGATCTTCTATGG	Cloning of *M. leprae rpoB*, reverse
MLRBWTF1	CAGTTCATGGATCAGAACAACCCTC	Introduction of point mutation at codons 507 and 508
MLRBWTF2	TGTCGGCGCTGGGCCCGGGTGGTTT	Introduction of point mutation at codon 526
MLRBWTF3	TTCGCACTACGGCCGGATGTGCCCG	Introduction of point mutation at codon 547
MLRBWTR1	CGACAGCTGGCTGGTGCCGAAGAAT	Introduction of point mutation at codons 513, 516, and 517
MLRBWTR2	GCCGGCGCTTGTGGGTCAGGCCCGA	Introduction of point mutation at codons 531, 532, and 533
MLRB507GGG	CGACAGCTGGCTGGTCCCGAAGAAT	Introduction of point mutation GGC507→GGG
MLRB507AGC	CGACAGCTGGCTGGTGCTGAAGAAT	Introduction of point mutation GGC507→AGC
MLRB508ACA	CGACAGCTGGCTTGTGCCGAAGAAT	Introduction of point mutation ACC508→ACA
MLRB513GTG	GTGTTCATGGATCAGAACAACCCTC	Introduction of point mutation CAG513→GTG
MLRB516AAT	CAGTTCATGAATCAGAACAACCCTC	Introduction of point mutation GAT516→AAT
MLRB517CAT	CAGTTCATGGATCATAACAACCCTC	Introduction of point mutation CAG517→CAT
MLRB526TAC	GCCGGCGCTTGTAGGTCAGGCCCGA	Introduction of point mutation CAC526→TAC
MLRB531TTG	TGTTGGCGCTGGGCCCGGGTGGTTT	Introduction of point mutation TCG531→TTG
MLRB531TGG	TGTGGGCGCTGGGCCCGGGTGGTTT	Introduction of point mutation TCG531→TGG
MLRB532TCG	TGTCGTCGCTGGGCCCGGGTGGTTT	Introduction of point mutation GCG532→TCG
MLRB533CCG	TGTCGGCGCCGGGCCCGGGTGGTTT	Introduction of point mutation CTG533→CCG
MLRB547ATC	GGGTGCACGTCACGGATCTCTAGCC	Introduction of point mutation GTC547→ATC
M. tuberculosis		
MTRBWTF	GCGAATTCTTGGCAGATTCCCGCCAGAG	Cloning of *M. tuberculosis rpoB*, forward
MTRBWTR	GCAAGCTTTTACGCAAGATCCTCGACAC	Cloning of *M. tuberculosis rpoB*, reverse
MTRBWTF1	AATTCATGGACCAGAACAACCCGCT	Introduction of point mutation at codons 507, 508, 510, 511, 512, and 513 and deletion of codons 506-508
MTRBWTF2	CTGTCGGCGCTGGGGCCCGGCGGTC	Introduction of point mutation at codons 522, 523, 526, and 531
MTRBWTR1	GGCTCAGCTGGCTGGTGCCGAAGAA	Introduction of mutation at codons 514, 516, 518, 519, and 521; deletion of codon 518; and insertion of TTC between codons 514 and 515
MTRBWTR2	TCGGCGCTTGTGGGTCAACCCCGAC	Introduction of point mutations TCG531→TTC and TCG531→TTG
MTRB507AGC	GGCTCAGCTGGCTGGTGCTGAAGAA	Introduction of point mutation GGC507→AGC
MTRB507GAT	GGCTCAGCTGGCTGGTATCGAAGAA	Introduction of point mutation GGC507→GAT
MTRB508CAC	GGCTCAGCTGGCTGTGGCCGAAGAA	Introduction of point mutation ACC508→CAC
MTRB508GCC	GGCTCAGCTGGCTGGCGCCGAAGAA	Introduction of point mutation ACC508→GCC
MTRB510CAT	GGCTCAGATGGCTGGTGCCGAAGAA	Introduction of point mutation CAG510→CAT
MTRB511CCG	GGCTCGGCTGGCTGGTGCCGAAGAA	Introduction of point mutation CTG511→CCG
MTRB513AAT1	TGCTCAGCTGGCTGGTGCCGAAGAA	Introduction of point mutation CAA513→AAT
MTRB513AAT2	ATTTCATGGACCAGAACAACCCGCT	Introduction of point mutation CAA513→AAT
MTRB513GAA	CGCTCAGCTGGCTGGTGCCGAAGAA	Introduction of point mutation CAA513→GAA
MTRB516GAG	AATTCATGGAGCAGAACAACCCGCT	Introduction of point mutation GAC516→GAG
MTRB516CAC	AATTCATGCACCAGAACAACCCGCT	Introduction of point mutation GAC516→CAC
MTRB516GTC	AATTCATGGTCCAGAACAACCCGCT	Introduction of point mutation GAC516→GTC
MTRB521ATG	AATTCATGGACCAGAACAACCCGAT	Introduction of point mutation CTG521→ATG
MTRB522TTG	TCGGCGCTTGTGGGTCAACCCCAAC	Introduction of point mutation TCG522→TTG
MTRB523GCG	TCGGCGCTTGTGGGTCAACGCCGAC	Introduction of point mutation GGG523→GCG
MTRB523GGC	TCGGCGCTTGTGGGTCAAGCCCGAC	Introduction of point mutation GGG523→GGC
MTRB526CTC	TCGGCGCTTGAGGGTCAACCCCGAC	Introduction of point mutation CAC526→CTC
MTRB526TAC	TCGGCGCTTGTAGGTCAACCCCGAC	Introduction of point mutation CAC526→TAC
MTRB526GAC	TCGGCGCTTGTCGGTCAACCCCGAC	Introduction of point mutation CAC526→GAC
MTRB526TTC	TCGGCGCTTGAAGGTCAACCCCGAC	Introduction of point mutation CAC526→TTC
MTRB526AAC	TCGGCGCTTGTTGGTCAACCCCGAC	Introduction of point mutation CAC526→AAC
MTRB526CGC	TCGGCGCTTGCGGGTCAACCCCGAC	Introduction of point mutation CAC526→CGC
MTRB526CAA	TCGGCGCTTTTGGGTCAACCCCGAC	Introduction of point mutation CAC526→CAA
MTRB529AAA	TTTGCGCTTGTGGGTCAACC	Introduction of point mutation CGA529→AAA
MTRB531TTC	CTGTTCGCGCTGGGGCCCGGCGGTC	Introduction of point mutation TCG531→TTC
MTRB531TTG	CTGTTGGCGCTGGGGCCCGGCGGTC	Introduction of point mutation TCG531→TTG
MTRB506d	GGCTCAGCTGGCTGAACTCCTTGAT	Introduction of mutation 506-508del
MTRBin514TTC	AATTCTTCATGGACCAGAACAACCC	Introduction of mutation 514insTTC
MTRBd518	AATTCATGGACCAGAACCCGCTGTC	Introduction of mutation 518del

[a] Restriction sites are underlined.

Downloaded from http://aac.asm.org/ on March 19, 2012 by NATL INST OF INFECTIOUS DISEAS

TABLE 2 Rifampin and rifabutin susceptibilities of the recombinant *M. smegmatis* strains

Mutation	Rifampin		Rifabutin		Reference(s)
	MIC (μg/ml)	Fold increase[a]	MIC (μg/ml)	Fold increase	
M. leprae					
Wild type	1		0.25		
GGC507→GGG (silent)	1	1	0.25	1	This study
GGC507→AGC (G507S)	0.5	0.5	0.125	0.5	3
ACC508→ACA (silent)	1	1	0.25	1	This study
CAG513→GTG (Q513V)	32	32	8	32	3
GAT516→AAT (D516N)	32	32	2	8	14
CAG517→CAT (Q517H)	1	1	0.25	1	11
CAC526→TAC (H526Y)	32	32	8	32	14
TCG531→TTG (S531L)	32	32	4	16	3, 14
TCG531→TGG (S531W)	32	32	8	32	14
GCG532→TCG (A532S)	1	1	0.25	1	11
CTG533→CCG (L533P)	32	32	4	16	14
GTC547→ATC (V547I)	1	1	0.25	1	This study
M. tuberculosis					
Wild type	1		0.25		
GGC507→AGC (G507S)	0.5	0.5	0.125	0.5	1
GGC507→GAT (G507D)	0.5	0.5	0.125	0.5	1
ACC508→CAC (T508H)	0.5	0.5	0.125	0.5	1
ACC508→GCC (T508A)	1	1	0.25	1	1
CAG510→CAT (Q510H)	1	1	0.25	1	22
CTG511→CCG (L511P)	16	16	1	4	1, 12
CAA513→AAT (Q513N)	8	8	0.5	2	1
CAA513→GAA (Q513E)	32	32	2	8	1
GAC516→GAG (D516E)	8	8	0.5	2	12
GAC516→CAC (D516H)	1	1	0.25	1	1
GAC516→GTC (D516V)	32	32	2	8	12, 21, 22
CTG521→ATG (L521M)	1	1	0.125	0.5	21
TCG522→TTG (S522L)	>32	>32	8	32	21
GGG523→GCG (G523A)	1	1	0.125	0.5	1
GGG523→GGC (silent)	1	1	0.25	1	1
CAC526→CTC (H526L)	32	32	4	16	12, 22
CAC526→TAC (H526Y)	>32	>32	8	32	12, 22
CAC526→GAC (H526D)	>32	>32	8	32	12, 22
CAC526→TTC (H526F)	>32	>32	4	16	1
CAC526→AAC (H526N)	32	32	2	8	8
CAC526→CGC (H526R)	32	32	8	32	12, 22
CAC526→CAA (H526Q)	8	8	0.5	2	1
CGA529→AAA (R529K)	32	32	4	16	22
TCG531→TTC (S531F)	32	32	4	16	1
TCG531→TTG (S531L)	32	32	8	32	21, 22
506-508del[b]	16	16	0.5	2	5
514insTTC[c]	>32	>32	8	32	12 22
518del[d]	32	32	2	8	22

[a] Fold increase in MIC compared to the wild-type sequence.
[b] Deletion of codons 506 to 508.
[c] Insertion of TTC between codons 514 and 515.
[d] Deletion of codon 518.

ic-exchange mutants were constructed by using a temperature-sensitive mycobacteriophage method described in a previous report (2). Using the *M. smegmatis* mc^{2}155 genome sequence (GenBank accession number CP000480), the upstream and downstream flanking DNA sequences were used to generate a deletion mutation in the *rpoB* gene (MSMEG_1367). To disrupt the *rpoB* gene, DNA segments from 1,119 bp upstream through 21 bp downstream of the initiation codon of *M. smegmatis rpoB* and from 39 bp upstream through 941 bp downstream of the termination codon were cloned directionally into the cosmid vector pYUB854, which contains a *res-hyg-res* cassette and a *cos* sequence for lambda phage assembly. The plasmids thus produced were digested with PacI and ligated into PH101 genomic DNA excised from the phage-plasmid hybrid (phasmid) phAE87 by PacI digestion. The ligated DNA was packaged (GigaPackIII Gold packaging extract; Stratagene, La Jolla, CA). The resultant mixture was used for the transduction of *E. coli* STBL2 cells (Life Technologies Inc., Carlsbad, CA) to yield cosmid DNA. After *E. coli* was transduced and the transductants were plated onto hygromycin-containing medium, phasmid DNA was prepared from the pooled antibiotic-resistant transductants and electroporated into *M. smegmatis* mc^{2}155. Bacterial cells were incubated at 30°C to produce the recombinant phage. The *M. smeg-*

Downloaded from http://aac.asm.org/ on March 19, 2012 by NATL INST OF INFECTIOUS DISEAS

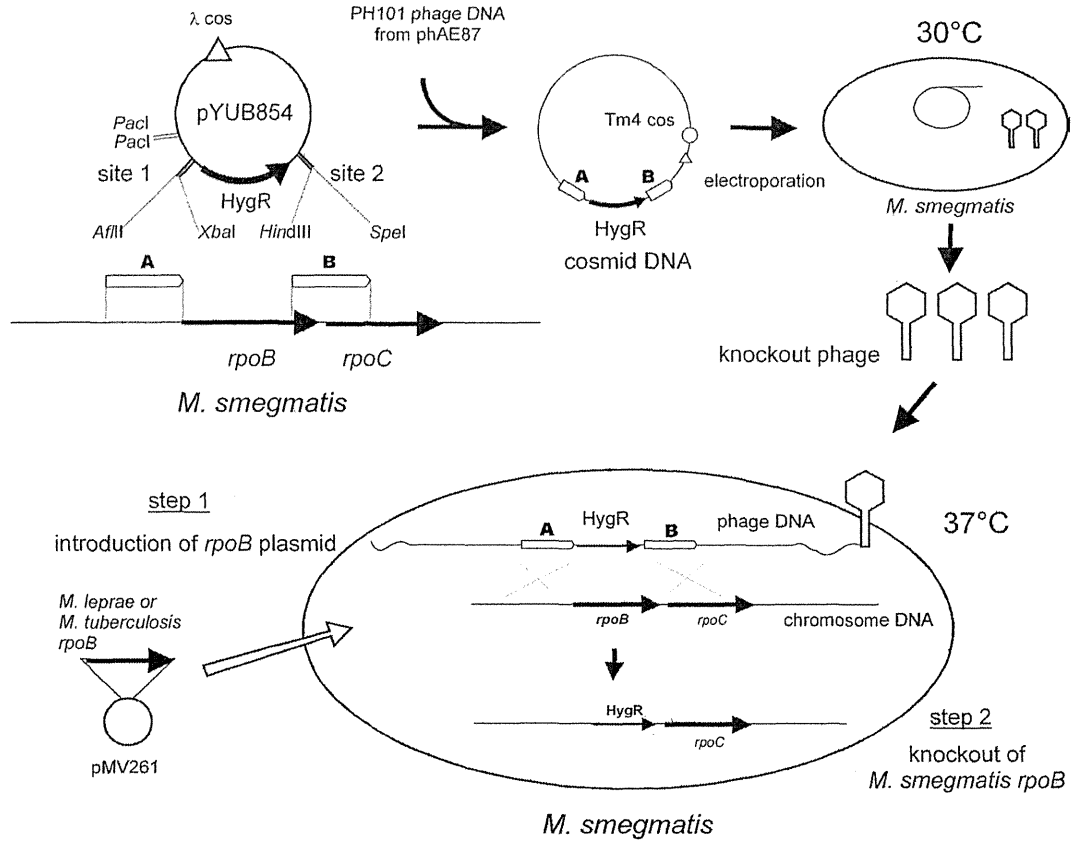

FIG 1 Construction of recombinant *M. smegmatis* strains for rifampin susceptibility testing.

matis transformant carrying the *M. leprae* or *M. tuberculosis rpoB* gene was infected with the produced temperature-sensitive phage at 37°C for allelic exchange, and kanamycin-resistant and hygromycin-resistant colonies were isolated. Two colonies for each point mutation were subjected to subsequent tests.

Drug susceptibility testing. The MIC values for *M. smegmatis* recombinant clones were determined by culture on Middlebrook 7H10 agar plates containing 2-fold serial dilutions of rifampin (0.25 to 32 μg/ml) or rifabutin (0.0625 to 8 μg/ml). The MIC value for each strain was defined as the lowest concentration of the drug necessary to inhibit bacterial growth.

RESULTS

Construction of recombinant *M. smegmatis* strains. In our previous study, we sequenced the *rpoB* regions of *M. leprae* clinical samples isolated in Vietnam and detected several mutations (11). In addition to these mutations, we detected some mutations (GGC→GGG at codon 507, ACC→ACA at codon 508, and GTC→ATC at codon 547) in clinical specimens from Vietnam and other countries (our unpublished data). We prepared plasmids with mutations in the *M. leprae* and *M. tuberculosis rpoB* genes. Each plasmid has one of 40 mutations (12 for *M. leprae rpoB* and 28 for *M. tuberculosis rpoB*) presented in Table 2. The mutated sequences were confirmed by sequencing. Plasmids carrying the *M. leprae* or *M. tuberculosis rpoB* gene with or without a point mutation were introduced individually into *M. smegmatis*. The *M. smegmatis* transformants were subjected to allelic exchange to disrupt the *rpoB* gene on their own chromosome (Fig. 1). The isolation of *rpoB*-disrupted mutants carrying the pNN301-*rpoB* constructs was unsuccessful. Consequently, the recombinant strains with pMV261-*rpoB* constructs were used for subsequent tests. PCR analysis confirmed that the *M. smegmatis rpoB* sequences in the recombinant strains with pMV261-*rpoB* constructs were replaced by hygromycin resistance gene sequences (see Fig. S1 in the supplemental material). All strains showed growth rates comparable to that of wild-type *M. smegmatis*.

Drug susceptibility. The rifampin susceptibilities and rifabutin susceptibilities of the recombinant *M. smegmatis* strains were tested (see Fig. S2 in the supplemental material). The MIC values of rifampin and rifabutin for the recombinant *M. smegmatis* strains and the fold increases in MIC compared to the wild-type sequences are presented in Table 2. It should be noted that the MIC values for the *M. smegmatis* strains might be shifted from those for *M. leprae* or *M. tuberculosis* because of their differences in cell wall permeability and other factors. The MIC value of rifampin for the recombinant *M. smegmatis* strain with the wild-type sequence of the *M. leprae rpoB* or *M. tuberculosis rpoB* gene was 1 μg/ml. Most strains that had a mutation at codon 511, 513, 516, 522, 526, 531, or 533 showed rifampin resistance. In contrast, strains that had a mutation at codon 507, 508, 517, 521, 523, or 532 showed MIC values of rifampin comparable to those for the wild-type sequence. The MIC values of rifabutin for the recombinant

Downloaded from http://aac.asm.org/ on March 19, 2012 by NATL INST OF INFECTIOUS DISEAS

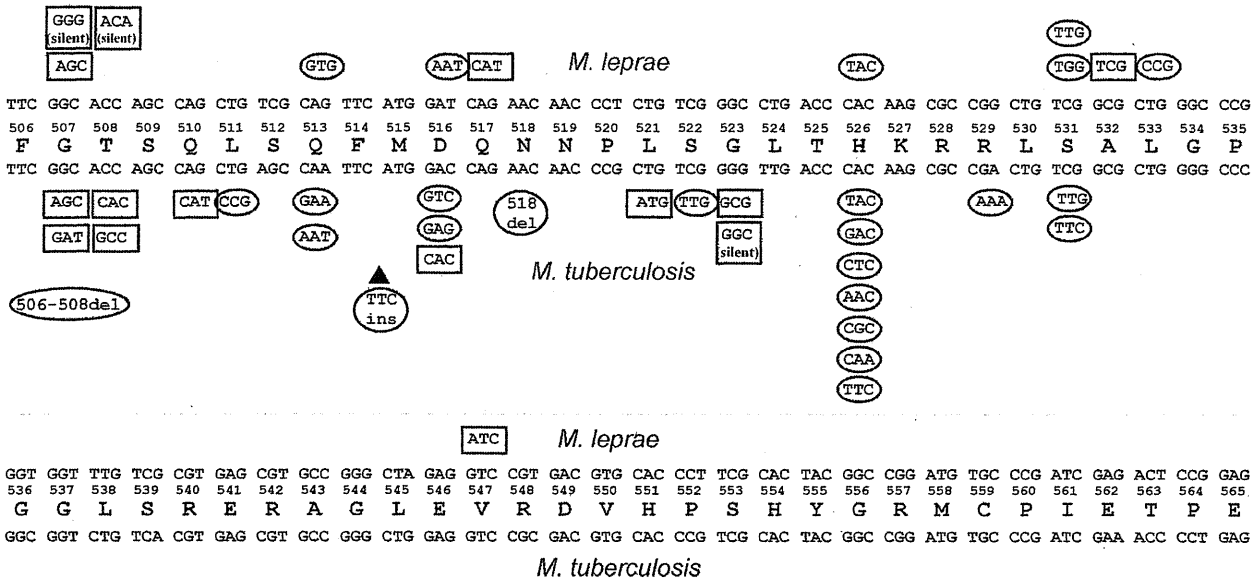

FIG 2 Mutations introduced into the *M. leprae rpoB* gene or *M. tuberculosis rpoB* gene and rifampin susceptibility. The consensus amino acid sequence of *M. leprae* RpoB and *M. tuberculosis* RpoB between codons 506 and 565 is shown. The *M. leprae rpoB* sequence and codons are shown above the consensus amino acid sequence. The *M. tuberculosis rpoB* sequence and codons are shown below the consensus sequence. Mutated codons that gave rise to rifampin resistance are surrounded by ovals. Mutated codons that showed levels of rifampin susceptibility comparable to those of the wild-type sequences are surrounded by rectangles.

M. smegmatis strains with the wild-type sequence of the *M. leprae rpoB* or *M. tuberculosis rpoB* gene were 0.25 μg/ml. Generally, rifabutin was more efficacious than rifampin in terms of concentration.

DISCUSSION

To functionally replace the *rpoB* gene of *M. smegmatis* with the *M. leprae* or *M tuberculosis* counterpart, we used a method established in our previous study (16). Because *rpoB* is a necessary gene for bacterial growth, this genetic locus cannot be disrupted without compensating for its activity. Therefore, we first introduced the *rpoB* gene of *M. leprae* or *M. tuberculosis* into *M. smegmatis* using vector plasmids of two types before disrupting the *rpoB* gene on the *M. smegmatis* chromosome. One vector was pMV261, a multicopy shuttle plasmid. The other was a single-copy integrative shuttle plasmid, pNN301. However, the isolation of *rpoB*-disrupted mutants carrying pNN301-*rpoB* constructs was unsuccessful, probably because of insufficient RpoB expression.

We tested 2 silent mutations and 10 mutations that change amino acid residues for *M. leprae* (Fig. 2). Codons 516, 526, 531, and 533 in the *M. leprae rpoB* gene are known to be codons responsible for rifampin resistance. However, it remains unclear whether or not mutations that have not been reported previously can confer rifampin resistance. Our results show that not all mutations in the *rpoB* gene detected in *M. leprae* clinical samples confer rifampin resistance. *M. leprae* is not cultivable. Therefore, it has been very difficult to analyze the mutation-susceptibility relationship. Using recombinant *M. smegmatis*, however, we can analyze it in a few weeks. We also tested 1 silent mutation, 24 mutations that change amino acids, 2 deletions, and 1 insertion for *M. tuberculosis*. Some mutations did not confer rifampin resistance, which is inconsistent with the susceptibility of the *M. tuberculosis* clinical isolates reported previously. Most mutations at codon 516, 526, or 531 showed rifampin resistance. It is interesting that the strains with the mutation GAC516→CAC for D516H were not rifampin resistant. All other mutations at codon 516 showed rifampin resistance. The mutation GAC516→CAC in *M. tuberculosis* was reported for a strain with multiple mutations and should not be involved in rifampin resistance.

Rifabutin, a spiropiperidyl rifampin, is a rifamycin derivative that is more active than rifampin against slow-growing mycobacteria, including *M. tuberculosis* and *M. avium-M. intracellulare* complex strains, *in vitro* and *in vivo*. It is also active against some rifampin-resistant strains of *M. tuberculosis* (6, 13). Our results indicate that some mutations (e.g., GAT516→AAT of *M. leprae* and GAC516→GAG of *M. tuberculosis*) show weak resistance to rifabutin.

Molecular methods designed to detect drug resistance have some limitations. In some cases, the identified mutations are not related to the acquisition of resistance. Caution is necessary when considering mutations, especially if the mutation detected in clinical isolates is not reported very often. For example, Q510H and L521M mutations were detected in rifampin-resistant *M. tuberculosis* isolates (21, 22), but our results suggest that these mutations are not responsible for rifampin resistance (Table 2). The method used for this study can directly assess the influence of designated mutations in *rpoB*. If the mutations can confer rifampin resistance, we can eliminate the possibility that genetic variation in some region other than *rpoB* on the chromosome of the clinical isolates is responsible for the resistance. Bahrmand et al. previously reported the high-level rifampin resistance of *M. tuberculosis* isolates with multiple mutations within the *rpoB* gene (1). Our method might also be useful for analyzing multiple mutations

Downloaded from http://aac.asm.org/ on March 19, 2012 by NATL INST OF INFECTIOUS DISEAS

detected in the *rpoB* gene of clinical isolates to determine the contribution of each single mutation to rifampin resistance.

ACKNOWLEDGMENTS

This work was supported by grants from the Ministry of Health, Labor, and Welfare (Emerging and Re-Emerging Infectious Diseases).

REFERENCES

1. **Bahrmand AR, Titov LP, Tasbiti AH, Yari S, Graviss EA.** 2009. High-level rifampin resistance correlates with multiple mutations in the rpoB gene of pulmonary tuberculosis isolates from the Afghanistan border of Iran. J. Clin. Microbiol. 47:2744–2750.
2. **Bardarov S, et al.** 2002. Specialized transduction: an efficient method for generating marked and unmarked targeted gene disruptions in *Mycobacterium tuberculosis, M. bovis* BCG and *M. smegmatis.* Microbiology **148**: 3007–3017.
3. **Cambau E, et al.** 2002. Molecular detection of rifampin and ofloxacin resistance for patients who experience relapse of multibacillary leprosy. Clin. Infect. Dis. 34:39–45.
4. **Cavusoglu C, Turhan A, Akinci P, Soyler I.** 2006. Evaluation of the Genotype MTBDR assay for rapid detection of rifampin and isoniazid resistance in *Mycobacterium tuberculosis* isolates. J. Clin. Microbiol. **44**: 2338–2342.
5. **Chikamatsu K, Mizuno K, Yamada H, Mitarai S.** 2009. Cross-resistance between rifampicin and rifabutin among multi-drug resistant *Mycobacterium tuberculosis* strains. Kekkaku **84**:631–633. (In Japanese.)
6. **Dickinson JM, Mitchison DA.** 1987. In vitro activity of new rifamycins against rifampicin-resistant M. tuberculosis and MAIS-complex mycobacteria. Tubercle **68**:177–182.
7. **Franzblau SG, Hastings RC.** 1988. In vitro and in vivo activities of macrolides against Mycobacterium leprae. Antimicrob. Agents Chemother. **32**:1758–1762.
8. **Hauck Y, Fabre M, Vergnaud G, Soler C, Pourcel C.** 2009. Comparison of two commercial assays for the characterization of rpoB mutations in *Mycobacterium tuberculosis* and description of new mutations conferring weak resistance to rifampicin. J. Antimicrob. Chemother. **64**:259–262.
9. **Honore N, Cole ST.** 1993. Molecular basis of rifampin resistance in *Mycobacterium leprae.* Antimicrob. Agents Chemother. 37:414–418.
10. **Huitric E, Werngren J, Jureen P, Hoffner S.** 2006. Resistance levels and rpoB gene mutations among in vitro-selected rifampin-resistant *Mycobacterium tuberculosis* mutants. Antimicrob. Agents Chemother. **50**:2860–2862.
11. **Kai M, et al.** 2011. Analysis of drug-resistant strains of *Mycobacterium leprae* in an endemic area of Vietnam. Clin. Infect. Dis. 52:e127–e132.
12. **Kapur V, et al.** 1994. Characterization by automated DNA sequencing of mutations in the gene (rpoB) encoding the RNA polymerase beta subunit in rifampin-resistant *Mycobacterium tuberculosis* strains from New York City and Texas. J. Clin. Microbiol. 32:1095–1098.
13. **Luna-Herrera J, Reddy MV, Gangadharam PR.** 1995. In-vitro and intracellular activity of rifabutin on drug-susceptible and multiple drug-resistant (MDR) tubercle bacilli. J. Antimicrob. Chemother. **36**:355–363.
14. **Maeda S, et al.** 2001. Multidrug resistant *Mycobacterium leprae* from patients with leprosy. Antimicrob. Agents Chemother. **45**:3635–3639.
15. **McClure WR, Cech CL.** 1978. On the mechanism of rifampicin inhibition of RNA synthesis. J. Biol. Chem. **253**:8949–8956.
16. **Nakata N, Kai M, Makino M.** 2011. Mutation analysis of the *Mycobacterium leprae* folP1 gene and dapsone resistance. Antimicrob. Agents Chemother. 55:762–766.
17. **Ramaswamy S, Musser JM.** 1998. Molecular genetic basis of antimicrobial agent resistance in *Mycobacterium tuberculosis*: 1998 update. Tuber. Lung Dis. **79**:3–29.
18. **Rattan A, Kalia A, Ahmad N.** 1998. Multidrug-resistant *Mycobacterium tuberculosis*: molecular perspectives. Emerg. Infect. Dis. **4**:195–209.
19. **Rigouts L, et al.** 2007. Newly developed primers for comprehensive amplification of the rpoB gene and detection of rifampin resistance in *Mycobacterium tuberculosis.* J. Clin. Microbiol. 45:252–254.
20. **Telenti A, et al.** 1993. Detection of rifampicin-resistance mutations in *Mycobacterium tuberculosis.* Lancet **341**:647–650.
21. **Williams DL, et al.** 1994. Characterization of rifampin-resistance in pathogenic mycobacteria. Antimicrob. Agents Chemother. **38**:2380–2386.
22. **Yang B, et al.** 1998. Relationship between antimycobacterial activities of rifampicin, rifabutin and KRM-1648 and *rpoB* mutations of *Mycobacterium tuberculosis.* J. Antimicrob. Chemother. **42**:621–628.

Downloaded from http://aac.asm.org/ on March 19, 2012 by NATL INST OF INFECTIOUS DISEAS

doi: 10.1111/j.1346-8138.2011.01355.x

CASE REPORT

Mycobacterium shigaense sp. nov., a novel slowly growing scotochromogenic mycobacterium that produced nodules in an erythroderma patient with severe cellular immunodeficiency and a history of Hodgkin's disease

Kazue NAKANAGA,[1] Yoshihiko HOSHINO,[1] Makiko WAKABAYASHI,[2] Noriki FUJIMOTO,[2] Enrico TORTOLI,[3] Masahiko MAKINO,[1] Toshihiro TANAKA,[2] Norihisa ISHII[1]

[1]Leprosy Research Center, National Institute of Infectious Diseases, Tokyo, [2]Department of Dermatology, Shiga University of Medical Science, Shiga, Japan; and [3]Regional Reference Center for Mycobacteria, Careggi University Hospital, Florence, Italy

ABSTRACT

A novel slow-growing scotochromogenic mycobacterium was isolated from skin biopsies from a patient with a history of Hodgkin's disease and severe cellular immunodeficiency as an opportunistic pathogen. Clinical characterization of these lesions revealed papules and nodules with pathological granuloma formation. Genotypic analysis using 16S rRNA misidentified this isolate as *Mycobacterium simiae*. However, multiple gene analysis using the internal transcribed spacer between the 16S and 23S rRNA genes, and the *rpoB* and *hsp65* genes revealed the presence of a novel mycobacterium. The antimicrobial susceptibility of this isolate was completely different from that of *M. simiae*. On the basis of these findings, we propose naming this new species *Mycobacterium shigaense* sp. nov., and conclude that multiple gene analysis is required for the appropriate diagnosis and treatment of non-tuberculous mycobacterial infections.

Key words: cellular immunodeficiency, *Mycobacterium shigaense* sp.nov., non-tuberculous mycobacteria, opportunistic infection.

INTRODUCTION

Non-tuberculous mycobacteria (NTM) have been well recognized as causative agents of human diseases. Recently, a number of new species have been added to the NTM. Some of these cause opportunistic infections in immunocompromised patients, not only those with AIDS, but also non-AIDS associated infections. Here, we report an additional new species of mycobacterium that caused cutaneous infection occurring as an opportunistic infection.

CASE REPORT

A 55-year-old Japanese male with a history of treatment of neck-oriented Hodgkin's disease in 2000, presented with erythema accompanied by generalized itching in 2005. The lesion persisted and worsened after treatment with a low dose of oral corticosteroids, resulting in erythroderma and scattered cutaneous nodules on the body trunk in 2007. On physical examination, he presented with itchy erythema over more than 90% of the total body surface (erythroderma) (Fig. 1a); scattered nodules on his chest, back and extremities (Fig. 1b); and multiple papules (Fig. 1c) on his back. He also presented with high-grade fever and slight lymphadenopathy of the neck and axilla. Cytomegalovirus (CMV) retinitis was diagnosed by ophthalmologists and several positive values of CMV antigen were detected at the end stage. His symptoms progressed, and after 2008 he was treated with ganciclovir or valganciclovir. Laboratory tests showed elevated levels of white blood cells ($10.2 \times 10^3/mm^3$; normal range [NR], $3.0–8.0 \times 10^3$) composed of 79.8% segmented neutrophils (NR, 40–74), 3.9% eosinophils (NR, 0–7), 11% lymphocytes (NR, 15–48) and 0% atypical lymphocytes, lactate dehydrogenase (295 IU/L; NR, 100–210), C-reactive protein (1.9 mg/dL; NR, <0.3), immunoglobulin E (188 498 IU/mL; NR, <400) and soluble interleukin-2 receptor (7470 U/mL; NR, 135–483). The platelet counts, liver and renal functions, serum immunoglobulin levels, complement values and angiotensin-converting enzyme were all within normal ranges. Antibodies against human T-lymphotropic virus-1 and HIV-1 were negative. Phenotypic analysis of peripheral lymphocytes revealed an increase in CD3 (95%; NR, 60–78%), T-cell receptors (TCR)-αβ (94%) and -γδ (1%), CD4 (93%; NR, 28–47) CD8 (3%; NR, 25–42) and CD19 (1%; NR, 6–16). Southern blot of peripheral lymphocytes revealed no monoclonal band. A tuberculin skin test for purified protein derivative was

Correspondence: Kazue Nakanaga, Ph.D., Department of Mycobacteriology, Leprosy Research Center, National Institute of Infectious Diseases, 4-2-1 Aoba-cho, Higashimurayama-shi, Tokyo 189-0002, Japan. Email: nakanaga@nih.go.jp

Received 24 April 2011; accepted 21 June 2011.

© 2011 Japanese Dermatological Association

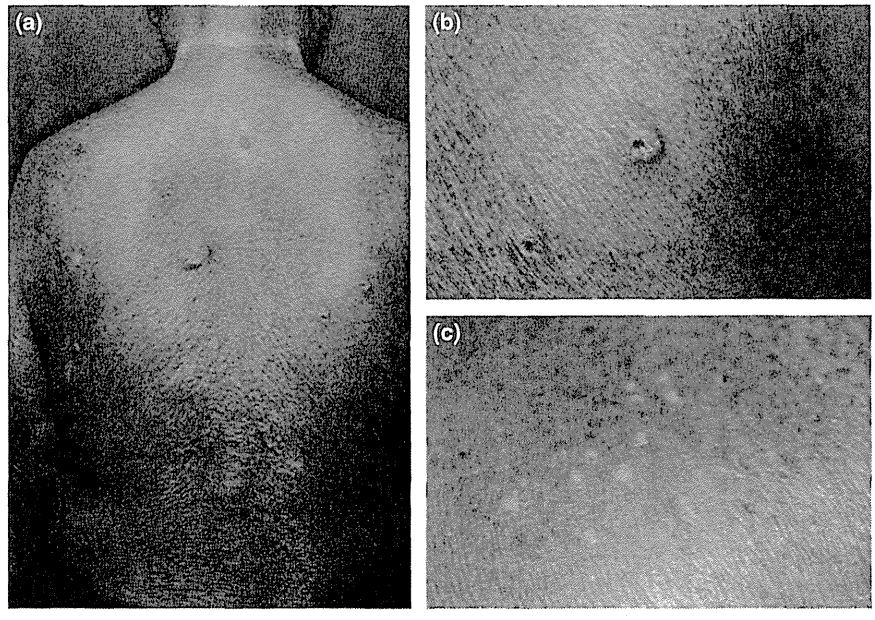

Figure 1. (a) Itchy erythema covered more than 90% of the body surface. (b) Scattered cutaneous nodules on the trunk. (c) Multiple papules on the back.

negative. A systemic investigation using computed tomography, endoscopy and Gallium scintigraphy revealed no abnormalities or internal malignancies, including a recurrence of Hodgkin's disease.

Skin biopsies were taken from the erythema, nodules and papules. A biopsy specimen from the erythema showed only lymphocytic infiltration (primarily CD4 T cells) around superficial dermal vessels (Fig. 2a). The lymphocytes were histologically normal, and Southern blot analysis of the biopsy specimen revealed no monoclonal band. The papules were histologically diagnosed as molluscum contagiosum (MC), because numerous basophilic inclusion bodies were observed in keratinocytes which located in the upper dermis. The nodular lesions showed dense infiltration of histiocytes in the superficial dermis, which formed granulomatous lesions (Fig. 2b). Ziehl–Neelsen staining of repeated biopsy specimens from these nodules showed multiple copies of banded acid-fast bacilli (Fig. 2c).

From these findings, we initially diagnosed an opportunistic mycobacterium infection in a patient of cellular immunodeficiency and administrated 400 mg of oral clarithromycin and 400 mg of isoniazid daily. The nodules improved within a few weeks. Multiple biopsies and histological investigations with Ziehl–Neelsen staining failed to detect any bacilli. The medicines were administrated for 12 months. New lesions of MC sometimes occurred after cessation of drug therapy, but no nodules were found. Oral prednisolone was administrated for the erythroderma. The erythroderma often recurred after healing of the mycobacterial infection, but because none of the skin biopsies from the erythroderma and peripheral blood showed atypical cells, the origin of the erythroderma is unknown.

While oral corticosteroids were effective, a daily low dose was needed to control the erythroderma. In October 2009, he complained of abdominal pain. At the time, he was almost blind due to CMV retinitis. Computed tomography showed a mass in the small

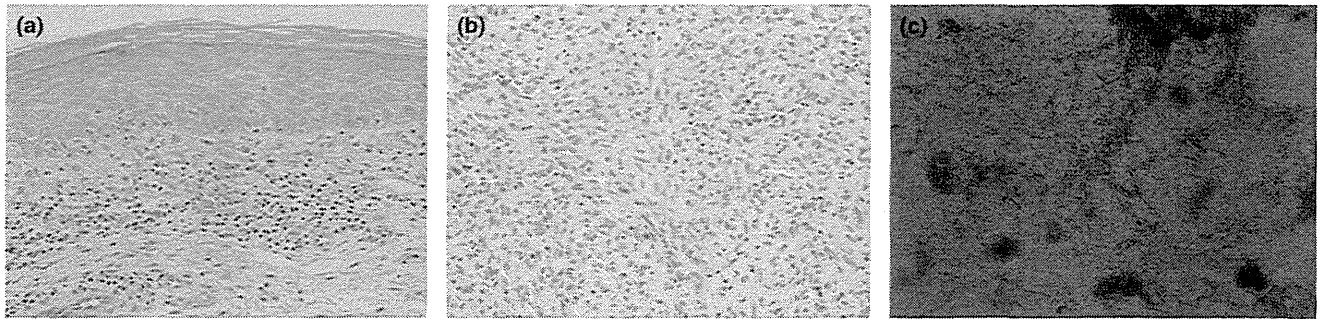

Figure 2. (a) Histological examination of erythema. Lymphocytic infiltration around superficial dermal vessels (hematoxylin–eosin [HE], original magnification ×100). (b) Histological examination of nodular lesions. Dense infiltrated histiocytes formed granulomatous lesions in the dermis (HE, ×200). (c) Ziehl–Neelsen staining of a skin biopsy from a nodule (oil immersion, ×1000).

© 2011 Japanese Dermatological Association

intestine and perforation of the gastrointestinal tract. Although a surgical resection of the mass in the small intestine was performed, he died of sepsis in November 2009. An autopsy was not performed. However, a histopathological examination of the mass revealed dense atypical lymphocytic infiltration without Hodgkin's cells, and Southern blot analysis showed a monoclonal band of TCR-αβ cells. Therefore, we concluded that he died not of a recurrence of Hodgkin's disease, but of non-Hodgkin T-cell lymphoma (NHL) with severe immunodeficiency.

A skin biopsy from the nodules confirmed multiple copies of acid-fast bacilli with Ziehl–Neelsen staining, although polymerase chain reaction (PCR) tests targeting *Mycobacterium tuberculosis*, *Mycobacterium avium*, *Mycobacterium intracellulare* and *Mycobacterium leprae* were all negative. The sequencing and genotypic analysis of DNA from the biopsy specimens using the first one-third of the16S rRNA gene showed the highest similarities to *Mycobacterium simiae* (99.54% identity with a 2-bp difference) and *Mycobacterium interjectum* (98.61% identity with a 6-bp difference) when compared with the Ribosomal Differentiation of Micro-organisms (RIDOM) database.[1]

The mycobacterium was isolated from the skin biopsy using the BBL MGIT tube (Becton Dickinson, Franklin Lakes, NJ, USA) and designated *Mycobacterium* sp. UN-152. Phenotypic characteristics were analyzed after sub-culturing on 2% Ogawa egg slant medium (Table 1).[2] The strain was scotochromogenic with an intense yellow color in both light and dark conditions and had a banded appearance after Ziehl–Neelsen staining (Fig. 3), however, usual strains of *M. simiae* are photochromogenic. The strain was slow-growing, had a smooth colonial morphology, and was positive for 3-day arylsulfatase activity, 68°C and semi-quantitative catalase activity

Table 1. Phenotypic differentiation between isolate *Mycobacterium* sp. UN-152 and genotypically similar species of mycobacteria

Characteristics	Isolate UN152 of *Mycobacterium* sp.	*Mycobacterium simiae* ATCC 25275^T	*Mycobacterium interjectum* ATCC 51457^T
Growth† in 7 days	+	+	+
Growth† at:			
25°C	+	+	+
30°C	+	+	+
37°C	+	+	+
42°C	−	+	−
Colony morphology	Smooth	Smooth	Smooth
Colony pigmentation			
In the dark	+	−	+
Photoactivity	−	+	−
Growth† supplemented with:			
PNB (500 μg/mL)	+	+	+
NaCl (5%)	+	+	+
TCH (1 μg/mL)	+	+	+
TCH (10 μg/mL)	+	+	+
Iron uptake	−	−	−
Niacin	−	+	−
Tween-80 hydrolysis (5, 10 days)	−	−	−
Urease	+	+	+
Nitrate reduction	−	−	−
Semi-quantitative catalase	+	+	+
68°C catalase	+	+	+
Arylsulfatase (3 day)	+	−	−
Pyrazinamidase	+	+	+
MPB64 production	−	−	−

†Bacterial growth was examined on 2% Ogawa slants.

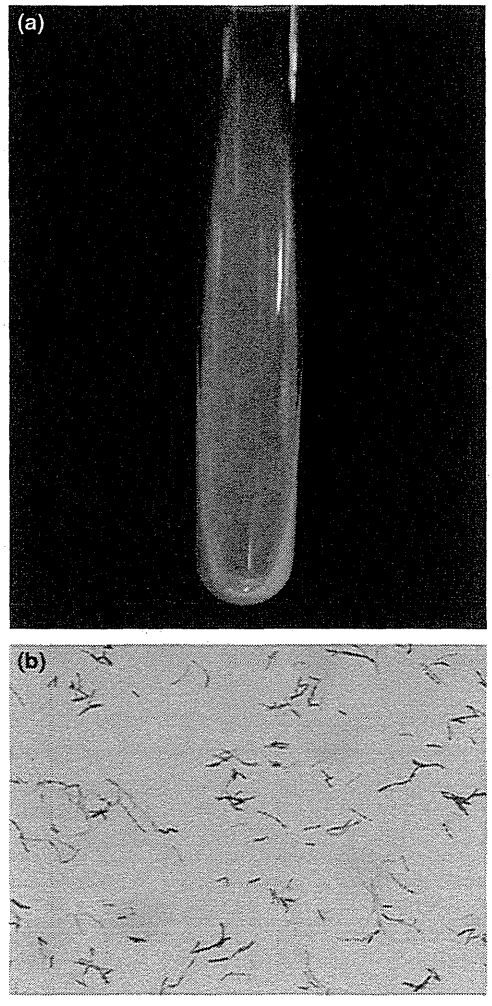

Figure 3. (a) Scotochromogenic colonies of *Mycobacterium* sp. UN-152 sub-cultured on 2% Ogawa egg medium. (b) Ziehl–Neelsen staining of *Mycobacterium* sp. UN-152 sub-cultured on 2% Ogawa egg medium (oil immersion, ×1000).

© 2011 Japanese Dermatological Association

and urease activity, but was negative for niacin activity, which suggested that this isolate was phenotypically different from *M. simiae*.

DNA–DNA hybridization to identify the species (DDH Mycobacteria Kyokuto Pharmaceutical Industrial, Tokyo, Japan) produced no matches with any of the 18 mycobacteria species included in the panel with *M. simiae*.[3] Further genotypic analysis was performed in an attempt to identify this isolate. Sequence analysis targeting fragments of the 16S rRNA gene, the internal transcribed spacer between the 16S and 23S rRNA genes (ITS region), and the *rpoB* and *hsp65* genes was performed (Table 2). Amplified PCR products were sequenced using an ABI Prism 310 PCR Genetic Analyzer (Applied Biosystems, Foster City, CA).[8] The sequences of isolate UN-152 were compared to those from the *M. simiae* (ATCC25275^T) type strain and the *M. simiae* clinical isolate 51808 from Japan.[9] We also performed a similarity search using BLAST to find identical and/or closely-related species of mycobacteria.[10] Phylogenetic analyses were performed using the neighbor joining method with Kimura's two-parameter distance correction model with 1000 bootstrap replications in the MEGA version 4.0.2 (Build#: 4028) software package.[11]

The sequence of the first one-third of the 16S rRNA gene from a sub-culture was identical with that from the previously examined skin biopsy. There were only four sites of a point difference between the sequence of UN-152 and that of *M. simiae* (99.7%

Table 2. Primers used in this study

Primer	Sequence	Target (amplified fragment size)	Reference
8F16S	5′-AGAGTTTGATCCTGGCTCAG-3′	16S rRNA gene (~1500 bp)	4
1047R16S	5′-TGCACACAGGCCACAAGGGA-3′		
830F16S	5′-GTGTGGGTTTCCTTCCTTGG-3′		
1542R16S	5′-AAGGAGGTGATCCAGCCGCA-3′		
ITSF	5′-TTGTACACACCGCCCGTC-3′	16S-23S ITS region (~340 bp)	5
ITSR	5′-TCTCGATGCCAAGGCATCCACC-3′		
MF	5′-CGACCACTTCGGCAACCG-3′	*rpoB* gene (351 bp)	6
MR	5′-TCGATCGGGCACATCCGG-3′		
TB11	5′-ACCAACGATGGTGTGTCCAT-3′	*hsp65* gene (441 bp)	7
TB12	5′-CTTGTCGAACCGCATACCCT-3′		

Table 3. DNA sequence similarities between isolate *Mycobacterium* sp. UN-152 and highly similar species of mycobacteria

	% identity			
Species†	16S rRNA (1471 bp)	ITS (280 bp)	*rpoB* (315 bp)	*hsp65* (401 bp)
Mycobacterium sp. UN-152	100	100	100	100
Mycobacterium simiae ATCC 25275^T	99.7	88.4	90.2	94.0
M. simiae 051808	99.7	88.4	90.8	94.0
Mycobacterium sherrisii ATCC BAA-832^T	99.5	ND	ND‡	93.0
Mycobacterium triplex ATCC 700071^T	99.1	85.7	ND	94.3
Mycobacterium cookii CIP 105396^T	ND	ND	95.9	93.3

†Sequence data (accession number in parenthesis) of three species were taken from database: *M. sherrisii* (AY353699, AY365190), *M. triplex* (U57632, GQ153291, AF334028) and *M. cookii* (AF547824, AY544904). ‡Not determined.

Table 4. Antibiotic susceptibility tests

	Minimal inhibitory concentration (μg/mL)		
Antibiotics	Isolate UN152 of *Mycobacterium* sp.	*Mycobacterium simiae* isolate	*M. simiae* (ATCC 25275T)
Streptomycin (SM)	8	16	4
Ethambutol (EB)	>128	32	44
Kanamycin (KM)	4	8	4
Isoniazid (INH)	>32	32	4
Rifampicin (REF)	0.03	>32	>32
Levofloxacin (LVFX)	0.5	2	1
Clarithromycin (CAM)	1	8	2
Ethionamide (TH)	>16	4	4
Amikacin (AMK)	4	8	4

© 2011 Japanese Dermatological Association

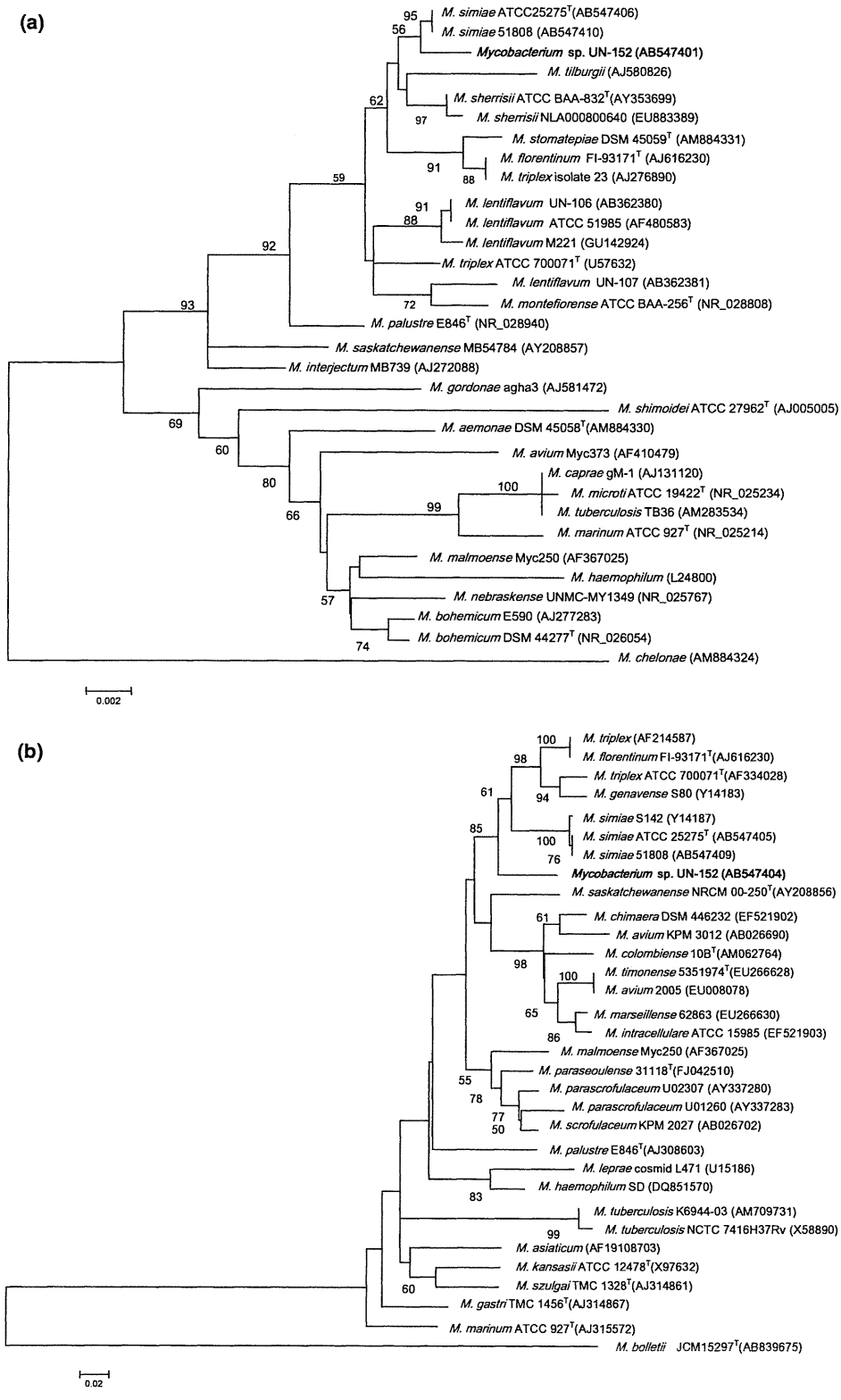

Figure 4. (a) Phylogenetic position of *Mycobacterium* sp. UN-152 (bold font) based on 1471 bp of the 16S rRNA gene. The percentages at the nodes represent bootstrap levels (values of <50% are not shown). The scale bar represents differences in nucleotide sequences. (b) Phylogenetic position of *Mycobacterium* sp. UN-152 (bold font) based on 280 bp of the 16S-23S rRNA ITS region. (c) Phylogenetic position of *Mycobacterium* sp. UN-152 (bold font) based on 315 bp of the *rpoB* gene. (d) Phylogenetic position of *Mycobacterium* sp. UN-152 (bold font) based on 401 bp of the *hsp65* gene.

© 2011 Japanese Dermatological Association

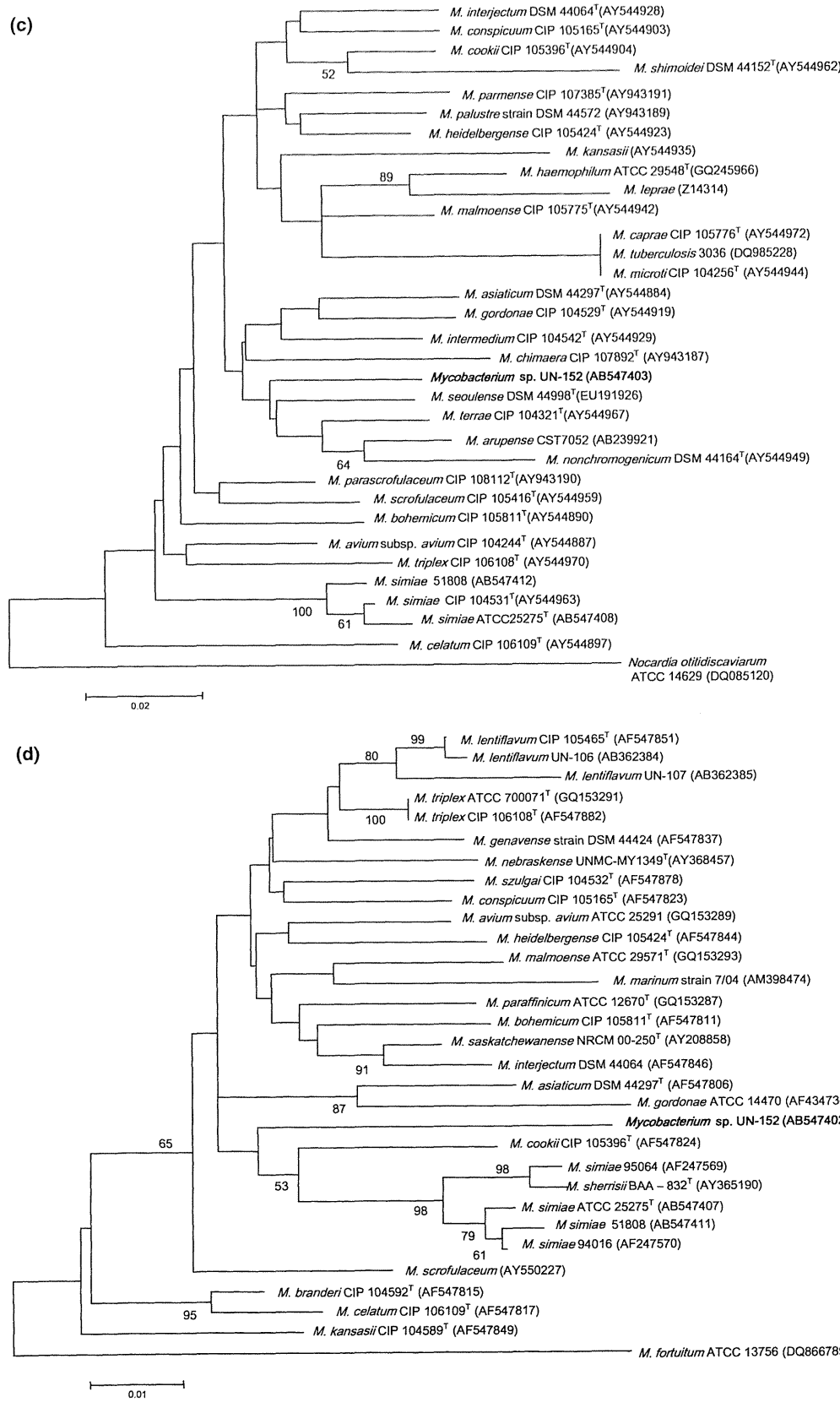

Figure 4. (*Continued*).

© 2011 Japanese Dermatological Association

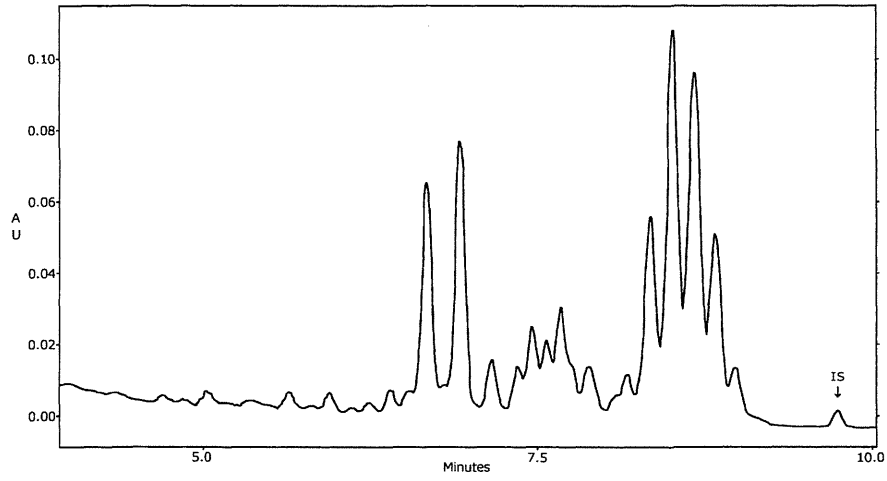

Figure 5. Mycolic acid analysis in *Mycobacterium* sp. UN-152 using high-performance liquid chromatography. IS, high molecular mass internal standard.

identity) when compared to almost all portions of the 16S rRNA gene (1471 bp). In contrast, the sequence identity of the ITS region was only 88. 4% between UN-152 and the *M. simiae*. *Mycobacterium cookii* revealed the highest similarity (95.9% identity) in the *rpoB* gene while *M. simiae* showed only 90.2–90.8% identities. *Mycobacterium triplex* exhibited the highest similarity in the *hsp65* gene (94.3% identity) while *M. simiae* was 94.0% similar (Table 3). However, there was no single mycobacterium species that showed the highest similarity across these four gene fragments, which suggested that this clinical isolate, *Mycobacterium* sp. UN-152, was a novel mycobacterium (Fig. 4).

Table 4 shows the results of antimicrobial susceptibility tests against *Mycobacterium* sp. UN-152, and the two strains of *M. simiae* (BrothMIC NTM; Kyokuto Pharmaceutical Industrial). *Mycobacterium* sp. UN-152 was highly susceptible to rifampicin and exhibited good susceptibility to clarithromycin and levofloxacin. Conversely, the minimal inhibitory concentration of rifampicin to *M. simiae* reference and clinical strains was more than 32 μg/mL, demonstrating that the antimicrobial susceptibility profile of the unknown isolate was different from that of *M. simiae*. The sequences obtained from the multiple gene analysis of the unknown clinical isolate (*Mycobacterium* sp. UN-152) and the *M. simiae* reference strains (ATCC25275^T and 51808) were deposited into the International Nucleotide Sequence Databases (INSD) through the DNA Databank of Japan (DDBJ)[12] under the accession numbers AB547401 to AB547412.

Finally, high-performance liquid chromatography of mycolic acid methyl esters was performed according to the CDC guidelines.[13] The pattern of bromophenacyl esters of mycolic acids can be used as an alternative method of discrimination of mycobacteria. The chromatographs revealed a representative profile characterized by three late clusters of peaks grossly resembling *M. simiae* or *Mycobacterium lentiflavum* (Fig. 5).[14]

DISCUSSION

Based on colony morphology, this clinical isolate may belong to NTM Runyon II. Because a slow-growing mycobacterium has a long culture time, the genotypic analysis of clinical samples would enable rapid diagnosis and treatment.[8,15] Genotypic analysis using the 16S rRNA gene is now contributing to diagnostics as an identification methodology for novel NTM.[16] In this case, the result of 16S rRNA gene sequences strongly suggested that *M. simiae* was the etiological strain; however, the identification was not supported by the scotochromogenic colony morphology and negative niacin accumulation. Additional sequence analysis targeting the ITS region and the *rpoB* and *hsp65* genes suggested the different species of mycobacteria, leading to the discovery of a novel NTM. We propose naming this new species *Mycobacterium shigaense* sp. nov.

Some species of recently registered mycobacteria may be of dubious clinical significance.[16] This isolate was determined to be clinically significant and not an environmental contaminant because: (i) it was isolated from multiple nodules, not from the erythema; (ii) the nodules improved after treatment with clarithromycin and isoniazid; and (iii) the isolate was no longer detectable once the nodules improved, a result which was repeatedly confirmed histologically. Unfortunately we could not know the source of this mycobacterium infection from medical interview.

In this case, MC infection was frequently seen in the trunk, CMV retinitis was diagnosed and treated for several months, and finally NHL was diagnosed. These findings were indicative of a significant cellular immunity deficiency because MC, CMV and NHL are frequently found in advanced AIDS patients with significant cellular immunodeficiency.[17–19] We propose that the decrease of peripheral CD8 T cells and the history of Hodgkin's disease resulted in severe immunodeficiency and that the cutaneous *M. shigaense* infection occurred as an opportunistic infection.

The genotypes obtained from a skin biopsy and subculture were identical, suggesting that the bacterium is responsible for the multiple nodules. In addition to the clinical significance, this case shows the insufficiency of single 16S rRNA gene analysis. Multiple gene analysis would be required to identify the species of mycobacteria.[20] This species has been never reported, but may have been previously misidentified as *M. simiae*. Because *M. shigaense* and *M. simiae* differ significantly in their susceptibility to rifampicin,

© 2011 Japanese Dermatological Association

clinicians must differentiate the two isolates in terms of the treatment. Therefore, multiple gene analysis that includes the ITS region and *rpoB* and *hsp65* genes is required for the appropriate treatment and diagnosis of NTM.

ACKNOWLEDGMENTS

We are indebted to Dr Tatsuo Kato (Nagara Medical Center) for giving us a clinical isolate of *Mycobacterium simiae* 51808. This work was supported in part by a Grant-in-Aid for Research on Emerging and Re-emerging Infectious Diseases from the Ministry of Health, Labor and Welfare of Japan to Y. H., M. M. and N. I. and by a Grant-in-Aid for Scientific Research (C) from the Ministry of Education, Culture, Sports, Science and Technology of Japan to Y. H.

REFERENCES

1 Turenne CY, Tschetter L, Wolfe J *et al.* Necessity of quality-controlled 16S rRNA gene sequence databases: identifying nontuberculous *Mycobacterium* species. *J Clin Microbiol* 2001; **39**: 3637–3648.
2 Della-Latta P, Weitzman I. Mycobacteriology. In: Isenberg HD, ed. *Essential Procedures for Clinical Microbiology*, 1st edn. Washington, DC: ASM Press, 1998; 169–203.
3 Kusunoki S, Ezaki M, Tamesada Y *et al.* Application of colorimetric microdilution plate hybridization for rapid genetic identification of 22 *Mycobacterium* species. *J Clin Microbiol* 1991; **29**: 1596–1603.
4 Springer B, Wu WK, Bodmer T *et al.* Isolation and characterization of a unique group of slowly growing mycobacteria: description of *Mycobacterium lentiflavum* sp. nov. *J Clin Microbiol* 1996; **34**: 1100–1107.
5 Roth A, Fischer M, Hamid ME *et al.* Differentiation of phylogenetically related slowly growing mycobacteria based on 16S–23S rRNA gene internal transcribed spacer sequences. *J Clin Microbiol* 1998; **36**: 139–147.
6 Kim B-J, Lee S-H, Lyu M-A *et al.* Identification of mycobacterial species by comparative sequence analysis of the RNA polymerase gene (*rpoB*). *J Clin Microbiol* 1999; **37**: 1714–1720.
7 Telenti A, Marchesi F, Balz M *et al.* Rapid identification of mycobacteria to the species level by polymerase chain reaction and restriction enzyme analysis. *J Clin Microbiol* 1993; **31**: 175–178.
8 Nakanaga K, Ishii N, Suzuki K *et al.* "*Mycobacterium ulcerans* subsp. *shinshuense*" isolated from a skin ulcer lesion: identification based on 16S rRNA gene sequencing. *J Clin Microbiol* 2007; **45**: 3840–3843.
9 Yoshimura K, Imao M, Goto H *et al.* A case of pulmonary infection due to *Mycobacterium simiae*. *Nihon Kokyuki Gakkai Zasshi* 2005; **43**: 32–36.
10 Altschul SF, Madden TL, Schaffer AA *et al.* Gapped BLAST and PSI-BLAST: a new generation of protein database search programs. *Nucleic Acids Res* 1997; **25**: 3389–3402.
11 Tamura K, Dudley J, Nei M *et al.* MEGA4: Molecular Evolutionary Genetics Analysis (MEGA) software version 4.0. *Mol Biol Evol* 2007; **24**: 1596–1599.
12 Kaminuma E, Mashima J, Kodama Y, *et al.* DDBJ launches a new archive database with analytical tools for next-generation sequence data. *Nucleic Acids Res 2010*; **38**: Database issue D33–D38.
13 Butler WR, Margaret MS, Floyd M, *et al.* Standardized method for HPLC identification of mycobacteria. 1996 [WWW document]. [cited 20 Apr, 2011] Available from URL: www.cdc.gov/ncidod/publications/hplc.pdf.
14 Tortoli E, Bartoloni A. High-performance liquid chromatography and identification of mycobacteria. *Rev Med Microbiol* 1996; **7**: 207–219.
15 Ishiwada N, Hishiki H, Watanabe M *et al.* Usefulness of PCR in rapidly diagnosing subcutaneous abscess and costal osteomyelitis caused by *Mycobacterium bovis* BCG. *Kansenshogaku Zasshi* 2008; **82**: 30–33.
16 Griffith DE, Aksamit T, Brown-Elliott BA *et al.* An official ATS/IDSA statement: diagnosis, treatment, and prevention of nontuberculous mycobacterial diseases. *Am J Respir Crit Care Med* 2007; **175**: 367–416.
17 Hoshino Y, Nagata Y, Gatanaga H *et al.* Cytomegalovirus (CMV) retinitis and CMV antigenemia as a clue to impaired adrenocortical function in patients with AIDS. *AIDS* 1997; **11**: 1719–1724.
18 Hoshino Y, Nagata Y, Taguchi H *et al.* Role of the cytomegalovirus (CMV)-antigenemia assay as a predictive and follow-up detection tool for CMV disease in AIDS patients. *Microbiol Immunol* 1999; **43**: 959–965.
19 Jung AC, Paauw DS. Diagnosing HIV-related disease: using the CD4 count as a guide. *J Gen Intern Med* 1998; **13**: 131–136.
20 Devulder G, Pérouse de Montclos M, Flandrois JP. A multigene approach to phylogenetic analysis using the genus Mycobacterium as a model. *Int J Syst Evol Microbiol* 2005; **55**: 293–302.

© 2011 Japanese Dermatological Association

International Immunology, Vol. 24, No. 10, pp. 637–644
doi:10.1093/intimm/dxs062
Advance Access publication 13 June 2012

© The Japanese Society for Immunology. 2012. All rights reserved.
For permissions, please e-mail: journals.permissions@oup.com

Critical role of AIM2 in *Mycobacterium tuberculosis* infection

Hiroyuki Saiga[1,2], Shoko Kitada[1], Yosuke Shimada[1,3], Naganori Kamiyama[1,3], Megumi Okuyama[1,3], Masahiko Makino[4], Masahiro Yamamoto[1,5,6,7] and **Kiyoshi Takeda[1,3,6]**

[1]Laboratory of Immune Regulation, Department of Microbiology and Immunology, Graduate School of Medicine, Osaka University, Suita, Osaka 565-0871, Japan
[2]The Association for Preventive Medicine of Japan, Koto-ku, Tokyo 135-0001, Japan
[3]Laboratory of Mucosal Immunology, WPI Immunology Frontier Research Center, Osaka University, Suita, Osaka 565-0871, Japan
[4]Department of Mycobacteriology, Leprosy Research Center, National Institute of Infectious Diseases, Higashimurayama, Tokyo 189-0002, Japan
[5]Laboratory of Immunoparasitology, WPI Immunology Frontier Research Center, Osaka University, Suita, Osaka 565-0871, Japan
[6]Core Research for Evolutional Science and Technology, Japan Science and Technology Agency, Saitama 332-0012, Japan
[7]Department of Immunoparasitology, Research Institute for Microbial Diseases, Osaka University, Suita, Osaka 565-0871, Japan

Correspondence to: K. Takeda; E-mail: ktakeda@ongene.med.osaka-u.ac.jp

Received 1 March 2012, *accepted* 9 April 2012

Abstract

Absent in melanoma 2 (AIM2) is a sensor of cytosolic DNA that is responsible for activation of the inflammasome and host immune responses to DNA viruses and intracellular bacteria. However, the role of AIM2 in host defenses against *Mycobacterium tuberculosis* is unknown. Here, we show that AIM2-deficient mice were highly susceptible to intratracheal infection with *M. tuberculosis* and that this was associated with defective IL-1β and IL-18 production together with impaired T_h1 responses. Macrophages from AIM2-deficient mice infected with *M. tuberculosis* showed severely impaired secretion of IL-1β and IL-18 as well as activation of the inflammasome, determined by caspase-1 cleavage. Genomic DNA extracted from *M. tuberculosis* (Mtb DNA) induced caspase-1 activation and IL-1β/IL-18 secretion in an AIM2-dependent manner. Mtb DNA, which was present in the cytosol, co-localized with AIM2. Taken together, these findings demonstrate that AIM2 plays an important role in *M. tuberculosis* infection through the recognition of Mtb DNA.

Keywords: host defense, inflammasome, macrophages

Introduction

Tuberculosis is caused by *Mycobacterium tuberculosis* and is a serious disease worldwide causing about 2 million deaths each year. The risk of disease is increased by the emergence of acquired immune deficiency syndrome and multidrug-resistant mycobacteria (1). *Mycobacterium tuberculosis* mainly invades and parasitizes macrophages by inhibiting phagosome maturation into phagolysosomes. Macrophages have several recognition systems to defend against mycobacterial invasion. Toll-like receptors (TLRs) recognize mycobacterial components such as glycolipids and CpG motif DNA (2–4). Several recent findings have also indicated that pattern recognition receptors other than TLRs, such as C-type lectin receptors and NOD-like receptors (NLRs), are implicated in the innate recognition of mycobacterial components (5–10). TLRs and C-type lectin receptors are membrane-bound molecules recognizing mycobacterial components in the extracellular compartments, whereas NLRs are present in the cytosol. Thus, several pattern recognition receptors showing distinct subcellular expression patterns recognize structurally and functionally different components of mycobacteria, contributing to protection by evoking an immune response.

Among the NLR family of proteins, NLR pyrin domain containing 3 (NLRP3) is known to activate the inflammasome, a multi-protein platform leading to the processing of the IL-1 family of cytokines (11–14). NLRP3 inflammasome, which is composed of NLRP3, adaptor protein Apoptosis-associated speck-like protein containing a CARD (ASC) and caspase-1, is activated by mycobacteria (15–18). Following activation, inactive caspase-1 is processed by autocleavage via ASC and is converted into the active form of caspase-1 containing

10 kDa/20 kDa subunits. The active form of caspase-1 then cleaves pro-IL-1β and pro-IL-18 into mature forms of IL-1β and IL-18, respectively. The IL-1 family of cytokines, including IL-1β and IL-18, possess potent pro-inflammatory activities (19–21) and are responsible for the host defense against mycobacteria (22–29). However, several studies suggest that NLRP3 or caspase-1, which mediates the processing of the IL-1 family of cytokines, is not essential for the induction of protective immunity to *M. tuberculosis in vivo* (25, 26, 30–32). Thus, the signaling pathway leading to IL-1β/IL-18 production in mycobacterial infection remains controversial.

Recent studies identified that AIM2 (absent in melanoma 2), which possesses HIN-200 and pyrin domains, recognizes cytosolic DNA leading to activation of the inflammasome and secretion of IL-1β and IL-18 (33–36). Several studies have demonstrated that AIM2 is mandatory for the host defense against DNA viruses (Vaccinia virus and mouse cytomegalovirus) and intracellular bacteria (*Francisella tularensis* and *Listeria monocytogenes*) (37–41). However, the role of AIM2-dependent inflammasome activation in mycobacterial infection remains unknown.

In this study, we analyzed the role of AIM2 in mycobacterial infection. AIM2-deficient mice were highly sensitive to *M. tuberculosis* infection. AIM2-deficient macrophages showed impaired activation of the inflammasome and defective production of IL-1β and IL-18 after *M. tuberculosis* infection. Genomic DNA from *M. tuberculosis* was present within the cytosol after infection and induced activation of the inflammasome in an AIM2-dependent manner. These findings demonstrate the critical role of AIM2 in *M. tuberculosis* infection.

Methods

Mice and bacteria

The *Aim2* gene was isolated from genomic DNA extracted from embryonic stem cells (V6.5) by PCR using Elongase Enzyme Mix (Invitrogen). The targeting vector was constructed by replacing a 2.5-kb fragment encoding the exons of *Aim2* with a neomycin-resistance gene cassette and a herpes simplex virus thymidine kinase gene driven by the PGK promoter for negative selection. After transfection of the targeting vector into embryonic stem cells, colonies resistant to both G418 and ganciclovir were selected and screened by PCR and Southern blot. Homologous recombinants were microinjected into blastocysts of C57BL/6 female mice, and heterozygous F1 progenies were intercrossed to obtain AIM2-deficient mice. AIM2-deficient mice and their wild-type littermates from these intercrosses were used and all animal experiments were conducted with the approval of the Animal Research Committee of the Graduate School of Medicine at Osaka University.

Mycobacterium tuberculosis strain H37Rv (ATCC358121) was grown in Middlebrook 7H9-ADC medium for 2 weeks and stored at –80°C until use.

In vivo infection of mice

Mice were intratracheally infected with *M. tuberculosis* H37Rv (1×10^6 CFU per mouse). At 4 weeks after infection, homogenates of the lungs and livers were plated onto 7H10-OADC agar. For histological analysis, the lungs were fixed with 4% PFA, embedded in paraffin, cut into sections, and stained with hematoxylin and eosin or by the Ziehl–Neelsen method.

Harvest of BALF, blood and cells from tissues

Bronchoalveolar lavage fluid (BALF) was collected from uninfected and infected mice by washing the lung airways with phosphate buffered saline (PBS) at 3 weeks post-infection, and blood was collected from the hearts of uninfected and infected mice. $CD4^+$ T cells (4×10^5 cells) were isolated from the spleens at 3 weeks after infection, and then were stimulated with PPD (2 μg ml^{-1}; Japan BCG Laboratory) in the presence of APC (4×10^5 cells) for 48 h.

Mycobacterium tuberculosis genomic DNA extraction

Mycobacterium tuberculosis (1×10^9 CFU) was homogenized with glass beads (0.1 mm; ASONE) and proteins were removed using Phenol/Chloroform/Isoamyl alcohol and Chloroform/Isoamyl alcohol. Genomic DNA was precipitated using isopropanol.

Cell culture and stimulation

Mice were intraperitoneally injected with 4% thioglycollate (Sigma) and 3 days later macrophages were isolated from the peritoneal cavity. Cells were stimulated with LPS (200 ng ml^{-1}) for 3 h and then transfected with poly(dA:dT) (Sigma) or *M. tuberculosis* DNA using Lipofectamine 2000 according to the manufacturer's instructions (Invitrogen). Peritoneal macrophages were infected with *M. tuberculosis* (MOI of 3) for 6 h. Cells were washed three times with PBS and then incubated for 24 h.

ELISA

The concentration of IFN-γ, IL-1β or IL-12p40 in culture supernatants was measured by ELISA according to the manufacturer's instructions (R&D Systems). The ELISA kit for IL-18 was purchased from Medical & Biological Laboratories.

Immuno-precipitation and immuno-blot analysis

Supernatants were precleared with protein G–Sepharose (GE Healthcare), incubated with anti-caspase-1 p10 rabbit antibody (2 μg; Santa Cruz Biotechnology). Cell pellets were lysed in lysis buffer (1% Nonidet P-40, 150 mM NaCl and 50 mM Tris-HCl, pH 7.5) and together with the immuno-precipitants, separated on SDS-PAGE and transferred to PVDF membranes (Millipore). The membranes were incubated with anti-caspase-1 p10 antibody (1:200) and anti-β-actin antibody (1:500; Sigma). Bound antibody was detected with SuperSignal West Dura Extended Duration Substrate (Thermo).

Immuno-fluorescence analysis

Mycobacterium tuberculosis genomic DNA was labeled with Hoechst 33342 (100 ng ml^{-1}; Invitrogen) by incubation for 24 h. Hoechst-labeled *M. tuberculosis* was washed five times with PBS before use. RAW264.7 cells were infected with Hoechst-labeled *M. tuberculosis* (MOI of 3) for 6 h, washed three times with PBS and then incubated for 24 h. Cells were fixed with 4% PFA and permeabilized with 0.4% saponin. The cells were incubated with rabbit anti-Rab7 antibody (1:200; Santa Cruz Biotechnology) or rabbit anti-AIM2 antibody (1:200; Santa Cruz Biotechnology) or rat anti-LAMP1 antibody (1:200; BD Biosciences) for 1 h at room temperature. Cells

were then incubated with Alexa 488 anti-rabbit IgG antibody (Invitrogen) or Alexa 594 anti-rat IgG antibody (Invitrogen) for 40 min at room temperature. The immuno-stained cells were mounted with ProLong Gold antifade reagent (Invitrogen) on glass slides and analyzed using a fluorescence microscope (FV1000-D IX81; Olympus).

Statistical analysis

Differences between control and experimental groups were evaluated using Student's *t* test. Values of $P < 0.05$ were considered to indicate statistical significance.

Results

Aim2$^{-/-}$ mice are highly susceptible to Mycobacterium tuberculosis infection

To assess the *in vivo* role of AIM2, we generated AIM2-deficient mice by gene targeting (Supplementary Figure 1A is available at *International Immunology* Online), which was confirmed by Southern and northern blot analyses (Supplementary Figure 1B and C is available at *International Immunology* Online). *Aim2$^{-/-}$* mice were born at normal Mendelian ratios, developed normally and showed no apparent abnormalities when housed in our specific pathogen-free facility. Several previous studies demonstrated that AIM2 recognizes cytosolic DNA, leading to caspase-1 activation and subsequent processing of the IL-1 family of cytokines, such as IL-1β and IL-18 (33–36, 39). Therefore, we first analyzed the response to synthetic B-form double-stranded DNA [poly(dA:dT)] in *Aim2$^{-/-}$* macrophages. Peritoneal macrophages were collected from wild-type and *Aim2$^{-/-}$* mice and then transfected with poly(dA:dT) into the cytosol after priming with LPS. In immuno-blot analysis, a 10 kDa active form of caspase-1 (p10) was detected in wild-type macrophages stimulated with poly(dA:dT). In contrast, the cleaved p10 form of caspase-1 was not detected in *Aim2$^{-/-}$* macrophages (Supplementary Figure 2A is available at *International Immunology* Online). In addition, poly(dA:dT)-induced secretion of IL-1β and IL-18 into the culture supernatants was markedly decreased in *Aim2$^{-/-}$* macrophages, although ATP-induced secretion of IL-1β was normally observed (Supplementary Figure 2B is available at *International Immunology* Online). Thus, in accordance with previous reports, *Aim2$^{-/-}$* mice showed defective DNA-induced activation of the inflammasome.

We examined the involvement of AIM2 in mycobacterial infection using these *Aim2$^{-/-}$* mice. Wild-type and *Aim2$^{-/-}$* mice were intratracheally infected with the virulent H37Rv strain of *M. tuberculosis* and monitored for their survival (Fig. 1A). All *M. tuberculosis*-infected wild-type mice survived to at least 8 weeks post-infection. In contrast, all *Aim2$^{-/-}$* mice died within 7 weeks of infection with *M. tuberculosis*. We also assessed bacterial burdens in the lungs and livers at 4 weeks post-infection (Fig. 1B). Colony-forming unit titers of *M. tuberculosis* in lungs and livers were higher in *Aim2$^{-/-}$* mice than in wild-type mice. We next performed histological analysis of the lungs of mice at 4 weeks post-infection. Gross appearances of the lungs of wild-type and *Aim2$^{-/-}$* mice were markedly different, and many granulomatous changes were evident in *M. tuberculosis*-infected *Aim2$^{-/-}$* mice (Fig. 2A). Hematoxylin and eosin staining

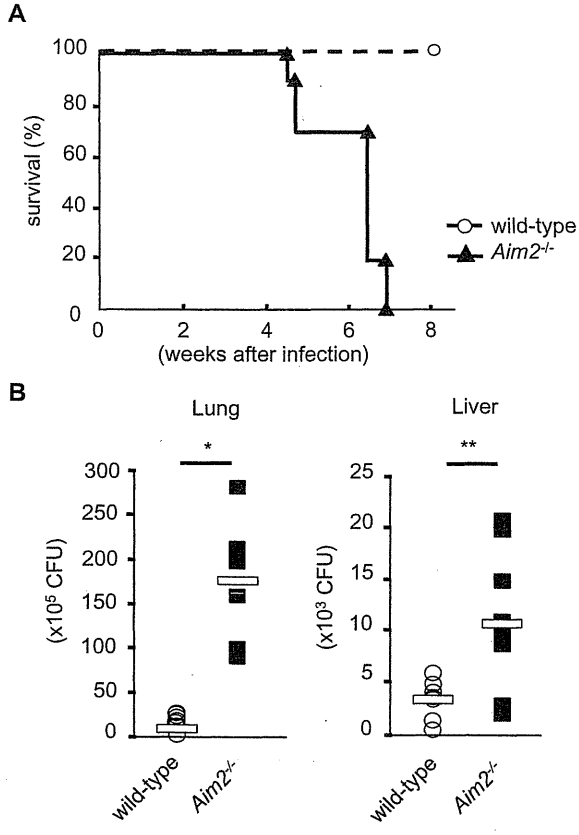

Fig. 1. *Aim2$^{-/-}$* mice are highly sensitive to infection with *M. tuberculosis*. (A) Wild-type ($n = 11$) and *Aim2$^{-/-}$* ($n = 10$) mice were intratracheally infected with *M. tuberculosis* and monitored for their survival. (B) Wild-type ($n = 7$) and *Aim2$^{-/-}$* ($n = 8$) mice were intratracheally infected with *M. tuberculosis*. At 4 weeks after infection, homogenates of the lungs and livers were plated onto 7H10-OADC agar and the CFU titers were counted. Symbols represent individual mice, and bars represent the mean CFU numbers. *, $P < 0.001$; **, $P < 0.01$.

of lung sections from infected *Aim2$^{-/-}$* mice demonstrated infiltration of many inflammatory cells (Fig. 2B). The number of *M. tuberculosis* in the lungs was measured by staining acid-fast bacilli using the Ziehl–Neelsen method (Fig. 2C). In the lungs of *Aim2$^{-/-}$* mice, the number of red-stained *M. tuberculosis* was markedly increased compared with those of wild-type mice. Taken together, these findings demonstrate that *Aim2$^{-/-}$* mice are highly susceptible to intratracheal infection with the virulent H37Rv strain of *M. tuberculosis*.

AIM2 mediates IL-1β/IL-18 production and T_h1 responses in Mycobacterium tuberculosis infection

Recent studies demonstrated that IL-1β is produced from *M. tuberculosis*-infected monocytes and alveolar macrophages mediating the host defense to mycobacteria (22–26, 42). Therefore, we first analyzed the levels of IL-1β in BALF from *M. tuberculosis*-infected mice (Fig. 3A). At 3 weeks after *M. tuberculosis* infection, IL-1β was abundantly detected in BALF from wild-type mice. In contrast, the concentration of IL-1β was profoundly decreased in BALF from *Aim2$^{-/-}$* mice. In addition to IL-1β, IL-18 has also been shown to be important for host resistance to mycobacterial infection (27–29). Therefore, we next

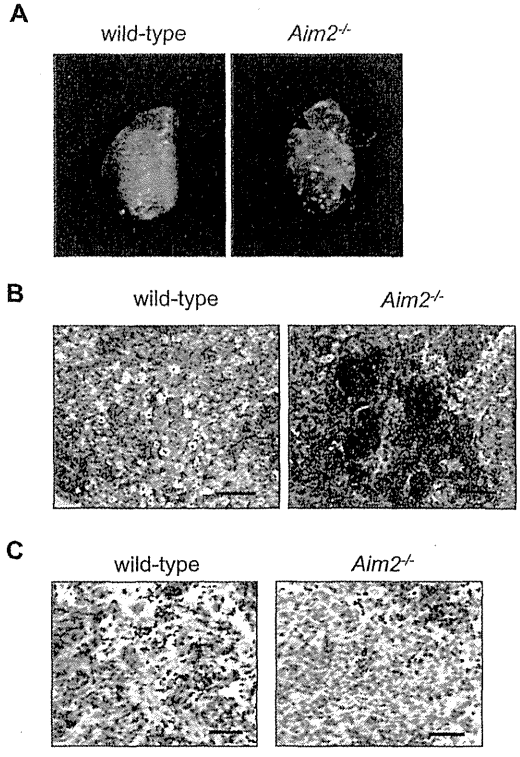

Fig. 2. High susceptibility of *Aim2*$^{-/-}$ mice to infection with *M. tuberculosis*. (A) Lung tissues from wild-type and *Aim2*$^{-/-}$ mice at 4 weeks post-intratracheal infection with *M. tuberculosis*. Arrows are shown to granulomatous lesion. (B) Lung tissue sections were stained with hematoxylin and eosin. Scale bars represent 100 μm. (C) Lung tissue sections were stained by the Ziehl–Neelsen method. Scale bars represent 40 μm.

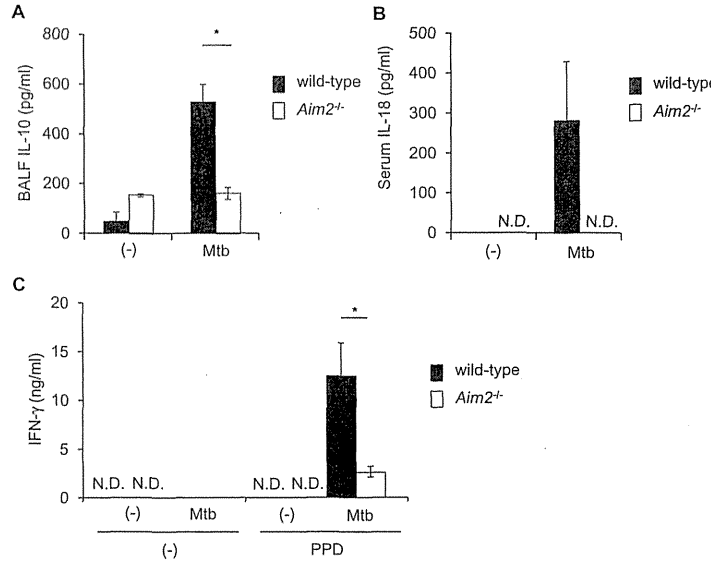

Fig. 3. Impaired production of IL-1β and IL-18 in *M. tuberculosis*-infected *Aim2*$^{-/-}$ mice. (A) BALF was collected from uninfected and infected mice at 3 weeks post-mycobacterial infection. BALF concentration of IL-1β was measured by ELISA. Data are presented as means ± SD of triplicate determinants and are one representative of two independent experiments. *, $P < 0.01$. (B) At 3 weeks after mycobacterial infection, sera were collected from uninfected and infected mice. Concentration of IL-18 was measured by ELISA. Data are presented as means ± SD of triplicate determinants and are one representative of two independent experiments. N.D., not detected. (C) CD4$^+$ T cells were isolated from the spleens of *M. tuberculosis*-uninfected and infected mice. The cells were co-cultured with APC for 48 h in the presence of PPD. The levels of IFN-γ in the cell supernatants were measured by ELISA. Data are presented as means ± SD of triplicate determinants and are one representative of two independent experiments. *, $P < 0.05$. N.D., not detected.

measured the serum levels of IL-18 in *M. tuberculosis*-infected mice (Fig. 3B). Serum concentration of IL-18 was increased in wild-type mice at 3 weeks post-infection. In contrast, IL-18 was not detected in sera from *M. tuberculosis*-infected *Aim2*$^{-/-}$ mice. We also assessed antigen-specific T_h1 responses following infection. CD4$^+$ T cells were isolated from the spleens of wild-type and *Aim2*$^{-/-}$ mice at 4 weeks post-infection and stimulated with a mycobacterial-specific antigen [purified protein derivative (PPD) of *Mycobacterium bovis*] in the presence of antigen-presenting cells (Fig. 3C). PPD stimulation induced marked production of IFN-γ in *M. tuberculosis*-infected wild-type mice. Antigen-specific production of IFN-γ was severely reduced in CD4$^+$ T cells derived from *M. tuberculosis*-infected *Aim2*$^{-/-}$ mice. These results indicate that the absence of AIM2 results in impaired production of IL-1β and IL-18 as well as T_h1 responses after *M. tuberculosis* infection.

AIM2 mediates Mycobacterium tuberculosis-induced inflammasome activation

We assessed the activation of caspase-1 to determine how AIM2-dependent immune responses develop following *M. tuberculosis* infection (Fig. 4A). Cleaved p10 form of caspase-1 was detected in *M. tuberculosis*-infected macrophages of wild-type mice. In contrast, cleavage of caspase-1 was severely reduced in *M. tuberculosis*-infected *Aim2*$^{-/-}$ macrophages.

We also analyzed cytokine production in *M. tuberculosis*-infected macrophages. Peritoneal macrophages from wild-type and *Aim2*$^{-/-}$ mice were infected with *M. tuberculosis* and the levels of cytokines in culture supernatants were measured by ELISA (Fig. 4B). *M. tuberculosis*-induced production of IL-12p40 or IFN-γ was comparable between wild-type and *Aim2*$^{-/-}$ macrophages. However, the production of IL-1β and IL-18 was severely reduced in *Aim2*$^{-/-}$ macrophages. Similar mRNA expression levels of *Il1b* and *Il18* in *M. tuberculosis*-infected wild-type and *Aim2*$^{-/-}$ macrophages were detected using real-time quantitative RT-PCR (Supplementary Figure 3 is available at *International Immunology* Online), indicating that AIM2 controls the production of IL-1β and IL-18 at the post-transcriptional level. Induction of *Ifnb*, encoding IFN-β, was enhanced in *M. tuberculosis*-infected *Aim2*$^{-/-}$ macrophages, confirming previous results (37). Thus, *M. tuberculosis*-infected *Aim2*$^{-/-}$ macrophages show defective caspase-1 activation leading to selective impairment in IL-1β and IL-18 secretion.

Mycobacterium tuberculosis genomic DNA activates AIM2 inflammasome

AIM2 has been shown to recognize cytosolic DNA (33–41). Therefore, we tested whether genomic DNA purified from